

## Carbon geochemistry of serpentinites in the Lost City Hydrothermal System (30°N, MAR)

Adélie Delacour<sup>a,\*</sup>, Gretchen L. Früh-Green<sup>a</sup>, Stefano M. Bernasconi<sup>b</sup>,  
Philippe Schaeffer<sup>c</sup>, Deborah S. Kelley<sup>d</sup>

<sup>a</sup> *Institute for Mineralogy and Petrology, ETH Zurich, CH-8092 Zurich, Switzerland*

<sup>b</sup> *Geological Institute, ETH Zurich, CH-8092 Zurich, Switzerland*

<sup>c</sup> *Laboratoire de Géochimie Bioorganique, UMR 7177 du CNRS, Université Louis Pasteur, Strasbourg, France*

<sup>d</sup> *School of Oceanography, University of Washington, Seattle, WA 98195, USA*

Received 18 June 2007; accepted in revised form 30 April 2008; available online 24 May 2008

### Abstract

The carbon geochemistry of serpentinitized peridotites and gabbroic rocks recovered at the Lost City Hydrothermal Field (LCHF) and drilled at IODP Hole 1309D at the central dome of the Atlantis Massif (Mid-Atlantic Ridge, 30°N) was examined to characterize carbon sources and speciation in oceanic basement rocks affected by long-lived hydrothermal alteration. Our study presents new data on the geochemistry of organic carbon in the oceanic lithosphere and provides constraints on the fate of dissolved organic carbon in seawater during serpentinization. The basement rocks of the Atlantis Massif are characterized by total carbon (TC) contents of 59 ppm to 1.6 wt% and  $\delta^{13}\text{C}_{\text{TC}}$  values ranging from  $-28.7\text{‰}$  to  $+2.3\text{‰}$ . In contrast, total organic carbon (TOC) concentrations and isotopic compositions are relatively constant ( $\delta^{13}\text{C}_{\text{TOC}}$ :  $-28.9\text{‰}$  to  $-21.5\text{‰}$ ) and variations in  $\delta^{13}\text{C}_{\text{TC}}$  reflect mixing of organic carbon with carbonates of marine origin. Saturated hydrocarbons extracted from serpentinites beneath the LCHF consist of *n*-alkanes ranging from  $\text{C}_{15}$  to  $\text{C}_{30}$ . Longer-chain hydrocarbons (up to  $\text{C}_{40}$ ) are observed in olivine-rich samples from the central dome (IODP Hole 1309D). Occurrences of isoprenoids (pristane, phytane and squalane), polycyclic compounds (hopanes and steranes) and higher relative abundances of *n*- $\text{C}_{16}$  to *n*- $\text{C}_{20}$  alkanes in the serpentinites of the southern wall suggest a marine organic input. The vent fluids are characterized by high concentrations of methane and hydrogen, with a putative abiotic origin of hydrocarbons; however, evidence for an inorganic source of *n*-alkanes in the basement rocks remains equivocal. We propose that high seawater fluxes in the southern part of the Atlantis Massif likely favor the transport and incorporation of marine dissolved organic carbon and overprints possible abiotic geochemical signatures. The presence of pristane, phytane and squalane biomarkers in olivine-rich samples associated with local faults at the central dome implies fracture-controlled seawater circulation deep into the gabbroic core of the massif. Thus, our study indicates that hydrocarbons account for an important proportion of the total carbon stored in the Atlantis Massif basement and suggests that serpentinites may represent an important—as yet unidentified—reservoir for dissolved organic carbon (DOC) from seawater.

© 2008 Elsevier Ltd. All rights reserved.

### 1. INTRODUCTION

Carbon is one of the most important elements and occurs in varying concentrations in the main reservoirs of the Earth: the mantle, the crust, the oceans, the atmosphere, and the biosphere. The speciation of carbon depends on the chemical and physical conditions prevailing in the reservoir, and its concentration and isotopic compo-

\* Corresponding author. Present address: Laboratoire de Géosciences Marines, Institut de Physique du Globe de Paris, 4 place Jussieu, 75252 Paris Cedex 5, France. Fax: +33 1 44 27 99 69.

E-mail address: [delacour@ipgp.jussieu.fr](mailto:delacour@ipgp.jussieu.fr) (A. Delacour).

sition reflect the dominant physical, chemical and/or biological processes in the system. In ridge environments, hydrothermal circulation of seawater through the oceanic crust and exposed mantle plays an integral part in the exchange of carbon between the lithosphere, the hydrosphere and the biosphere and has important consequences for global bio-geochemical cycles (Fig. 1).

Carbon in mantle rocks occurs predominantly as CO, CO<sub>2</sub>, and CH<sub>4</sub> in fluid inclusions or as solid phases in the form of graphite, carbonate, and organic compounds (Fig. 1). Mantle rocks show a bimodal distribution of carbon isotope compositions with the majority clustering around -5‰ and a minor component between -22‰ and -26‰ (Pineau and Javoy, 1983; Mathez, 1987; Deines, 2002; see Table 3 in Kelley and Früh-Green, 1999). The oceans contain two main pools of carbon: dissolved inorganic carbon (DIC) mainly present as bicarbonate (HCO<sub>3</sub><sup>-</sup>) with a δ<sup>13</sup>C of ~0‰ (Zeebe and Wolf-Galdrow, 2001); and organic carbon consisting of dissolved organic carbon (DOC; <0.45 μm diameter) with δ<sup>13</sup>C in the range of -18‰ to -23‰ (Druffel et al., 1992) and particulate organic carbon (POC; >0.45 μm diameter) with δ<sup>13</sup>C varying between -20‰ and -30‰ (Des Marais, 2001). Fluid circulation and alteration of the oceanic crust is accompanied by an uptake of carbon and by precipitation of carbonate veins whose abundance is proportional to the age of the crust (Hart et al., 1994; Alt and Teagle, 1999).

Volatiles are crucial elements that link geodynamic, geologic, and geo-biological processes on Earth. Degassing of volatiles is responsible for the formation of the early oceans and atmosphere (Kasting et al., 1993; Holland, 2002) and

influences the geochemical, deformational, and eruptive history of volcanoes. CO<sub>2</sub>, H<sub>2</sub>, CH<sub>4</sub>, H<sub>2</sub>S, and He are also key tracers to detect seafloor eruptive events and hydrothermal activity on the seafloor (e.g., Lilley et al., 1993; Fornari and Embley, 1995; Lupton, 1995; German and Von Damm, 2003 and references therein; Kelley et al., 2004). In addition, numerous studies have shown that the migration of volatiles through the oceanic crust plays a critical role in sustaining microbial communities in subsurface and near-vent environments (e.g., Deming and Baross, 1993; Baross and Deming, 1995; Fisher, 1995; Karl, 1995; Delaney et al., 1998; Kelley et al., 2004).

In most fast-spreading ridge environments, magmatic volatiles constitute major sources of energy for biological activity. In contrast, slow-spreading ridges are characterized by zones of low magmatic supply, in which relatively rapid unroofing and alteration of mantle and deep hot crustal rocks are significant processes in crustal development. In these environments, migration of seawater along deeply penetrating fault systems may facilitate hydration of the plutonic crust and serpentinize the upper mantle, leading to significant production of CH<sub>4</sub> and H<sub>2</sub> that provide important energy sources for microbial activity (Fig. 1).

Along the Mid-Atlantic Ridge (MAR), the Rainbow, Logatchev/Ashadze, Lost City and Saldanha hydrothermal fields are the only known seafloor hydrothermal systems hosted by variable mixtures of serpentinized peridotite and gabbroic material. These fields have fluid chemistries clearly distinct from basalt-hosted systems and are characterized by particularly high concentrations

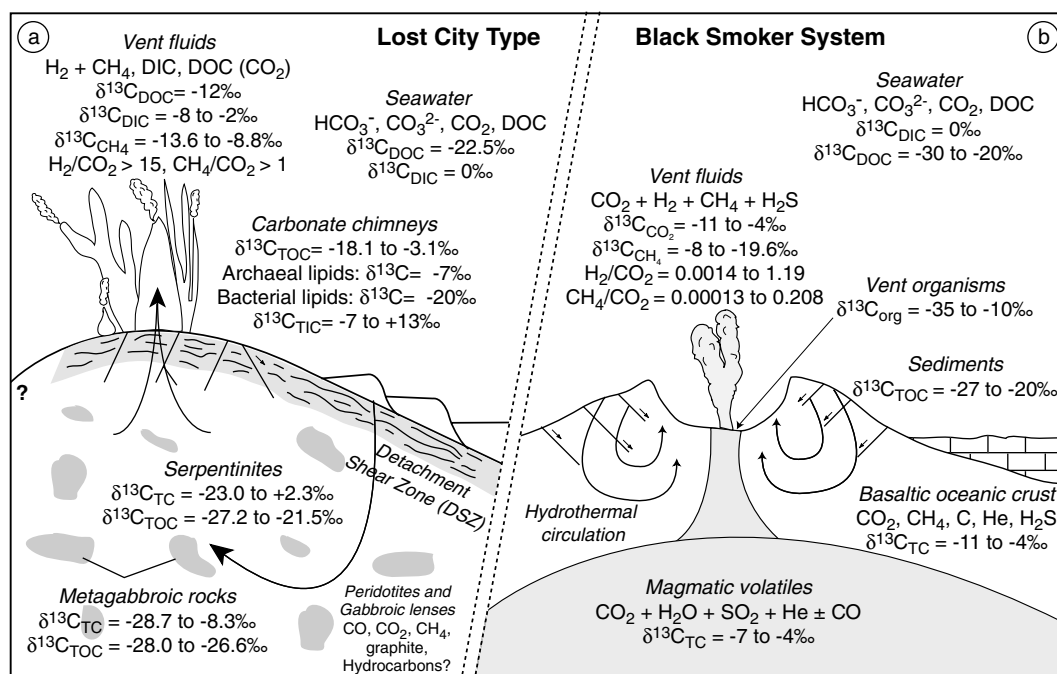


Fig. 1. Schematic representation of the carbon species and carbon isotope compositions of different reservoirs involved in hydrothermal systems at mid-ocean ridge environments. (a) Lost City-type hydrothermal system. Data are from Kelley et al. (2005), Lang et al. (2005), and our study. (b) Black smoker type system. Data are from Shanks et al. (1995), Charlou et al. (2002) and Kelley et al. (2004). Abbreviations: DOC, dissolved organic carbon; DIC, dissolved inorganic carbon; TOC, total organic carbon; TIC, total inorganic carbon; TC, total carbon.

of  $H_2$ ,  $CH_4$  and higher hydrocarbons related to serpentinization (e.g., Rona et al., 1987; Krasnov et al., 1995; Donval et al., 1997; Douville et al., 1997; Sagalevich et al., 2000; Holm and Charlou, 2001; Kelley et al., 2001, 2005; Proskurowski et al., 2008).  $H_2$  and  $CH_4$  anomalies in the water column are also observed above outcrops of serpentinized peridotites along the MAR and in highly tectonized areas away from the neovolcanic zones that are believed to be ultramafic in composition (e.g., Rona et al., 1987; Charlou et al., 1991; Rona et al., 1992; Bougault et al., 1993; Charlou and Donval, 1993; Charlou et al., 1998; Gracia et al., 2000; German and Von Damm, 2003). The discovery of  $H_2$ - and  $CH_4$ -rich, high pH fluids venting from carbonate-brucite towers at the Lost City Hydrothermal Field (LCHF) at the southern part of the Atlantis Massif (Fig. 2a) (Kelley et al., 2001) has particularly stimulated interest in serpentinization in off-axis environments. These volatiles sustain dense microbial communities, which include methanogenic and/or methanotrophic *Archaea*, methane-oxidizing bacteria, and sulfur-oxidizing and sulfate-reducing bacteria (Kelley et al., 2005; Brazelton et al., 2006). The Lost City hydrothermal system offers a unique opportunity to study the role of active serpentinization in generating volatile-rich fluids, in the uptake of carbon during hydrothermal alteration, and in the biological communities that may be supported in alkaline environments (Fig. 1).

In this paper, we present an isotopic and organic geochemical study of carbon in the basement rocks of the Atlantis Massif recovered by submersible below LCHF and by drilling of the Integrated Ocean Drilling Program (IODP) at Site U1309,  $\sim 5$  km to the north. These data are used to characterize carbon speciation and sources of carbon in peridotite-hosted hydrothermal systems. This study contributes new data on the geochemistry of organic carbon in serpentinites and gabbroic rocks affected by long-lived hydrothermal alteration and provides constraints on the fate of dissolved organic carbon in seawater during serpentinization and alteration of the oceanic lithosphere.

## 2. FORMATION AND ALTERATION OF THE ATLANTIS MASSIF

Located at  $30^\circ N$  along the Mid-Atlantic Ridge (MAR), the Atlantis Massif (AM) is a 1.5–2 Myr old dome-like massif forming the inside corner of the intersection between the MAR and the Atlantis Transform Fault (ATF; Fig. 2a). The massif is interpreted as an oceanic core complex (OCC), comprised of lower crustal and upper mantle rocks that were uplifted and exposed by low-angle detachment faulting (Cann et al., 1997; Blackman et al., 1998, 2002; Karson et al., 2006). Three domains are distinguished on the basis of lithologic and morphologic criteria: the gabbroic central dome, the peridotite-dominated southern wall

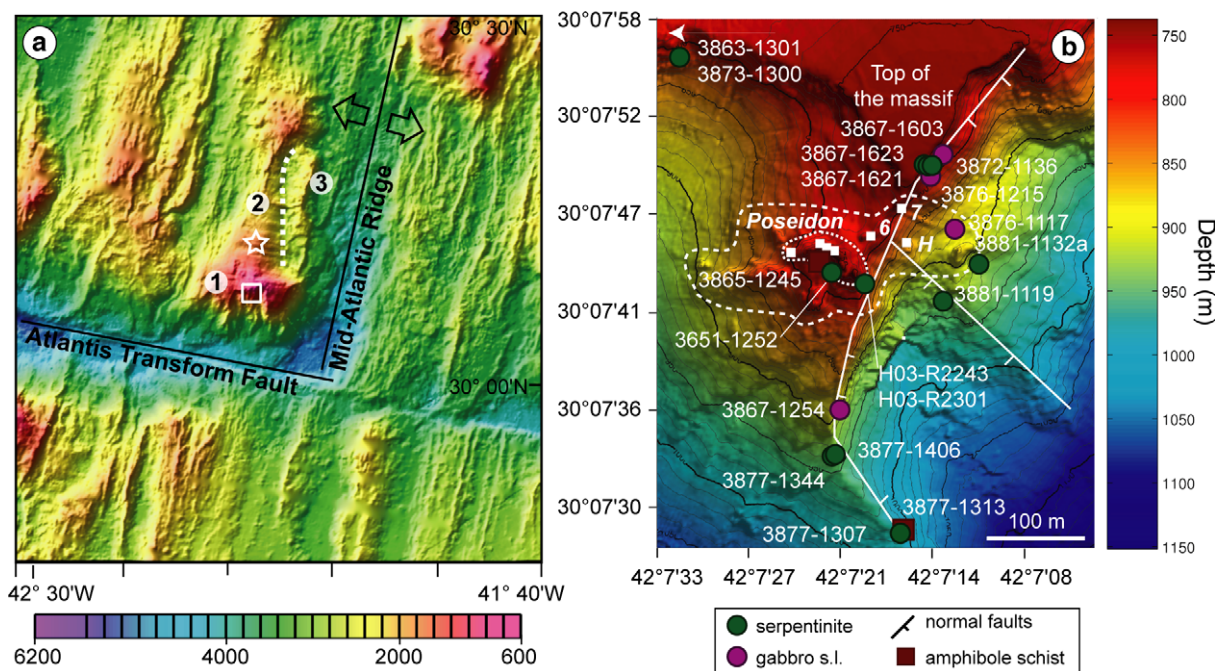


Fig. 2. (a) Location map and morphology of the Atlantis Massif at the inside corner of the intersection between the slow-spreading Mid-Atlantic Ridge and the Atlantis Transform Fault. The Atlantis Massif is divided into: (1) the peridotite-dominated southern wall, (2) the gabbroic central dome, and (3) the volcanic eastern block. The white box shows the study area of the southern part of the Atlantis Massif and the Lost City Hydrothermal Field, which is shown in detail in Fig. 2b. White star indicates the location of IODP Site U1309. (b) High resolution map of the Lost City Hydrothermal Field (LCHF) obtained by the autonomous vehicle ABE and gridded at 2 m (Kelley et al., 2005). The external dashed line shows the spatial extent of the LCHF, whereas the internal line indicates the size of the 60 m high hydrothermal structure Poseidon. Positions of the active chimneys, markers 6, H and 7 are given as white solid squares, as well as the location of normal faults (hatched lines) proposed by Karson et al. (2006) and the location of the samples analyzed for this study.

and the basaltic eastern block (Fig. 2a), which is interpreted as the hanging wall of the OCC. The surface of the massif is covered by pelagic sediments, rubble, and sedimentary breccias (Blackman et al., 2002; Schroeder et al., 2002; Früh-Green et al., 2003; Karson et al., 2006).

Site U1309, located at 1650 m water depth on the crest of the central dome (Fig. 2a), was drilled during IODP Expeditions 304 and 305 (Expedition Scientific Party, 2005a,b; Blackman et al., 2006) and consists of two deep holes (Holes 1309D and Hole 1309B) and five shallow penetration holes (Hole 1309A and Holes 1309E–H). Hole 1309D was drilled to 1415.5 m below the sea floor (mbsf; average core recovery 75%) and recovered predominantly gabbroic rocks (91.4% of total recovery) with minor intercalated ultramafic rocks (5.7% of total recovery; Expedition Scientific Party, 2005a,b; Blackman et al., 2006). The gabbroic rocks are compositionally diverse and comprise gabbro, olivine gabbro/troctolitic gabbro, troctolite, and oxide gabbro. Ultramafic lithologies are mainly olivine-rich troctolites with a poikilitic texture; mantle peridotites are rare (<0.3% of the recovery) and are concentrated in the upper part of Hole 1309D (<225 m).

Alteration in the gabbroic rocks at the central dome decreases downhole and is dominated by greenschist metamorphic conditions (<500 °C) with only minor deformation recorded under granulite- to amphibolite-facies conditions. Strontium and sulfur isotope compositions of samples from Hole 1309D (Delacour et al., 2006, 2008a) are locally elevated towards seawater-like values in the upper 800 m of the core and correlate with higher degrees of serpentinization of olivine-bearing rocks (e.g., harzburgite and troctolite). Below this depth, the gabbroic and ultramafic rocks preserve magmatic Sr- and S-isotope compositions. A predominance of Ni-rich and low-sulfur sulfide assemblages in the serpentinites and olivine-rich troctolites at the bottom of the hole reflect reducing conditions and relatively limited interaction with seawater restricted to narrow fault zones at depth (Delacour et al., 2008a).

The southern Atlantis Massif, ~5 km south of the central dome, is cut by steep normal faults, which together with mass wasting expose a near vertical, 3800 m high scarp north of the ATF (Fig. 2b). Submersible and dredging sampling along this scarp recovered primarily serpentinized ultramafic rocks (~70%) with interspersed gabbroic bodies (~30%; Blackman et al., 2002; Schroeder and John, 2004; Boschi et al., 2006; Karson et al., 2006). The peridotites are primarily depleted spinel harzburgites and are affected by a high degree of serpentinization (from 70% to 100%). Bulk rock oxygen isotope compositions are generally depleted in  $^{18}\text{O}$  ( $\delta^{18}\text{O}$  values from +1.7‰ to +5.5‰ V-SMOW) and indicate that alteration was most pervasive at temperatures of ~150–250 °C (Boschi et al., 2008). A lack of Fe–Ni alloys, the predominance of magnetite, and very low amounts of pyrite in the serpentinites reflect slightly oxidizing conditions during serpentinization (Delacour et al., 2005, 2007). Seawater-like S-, Sr-, and Nd-isotope compositions of serpentinites at the southern wall indicate very high fluid–rock ratios (>20 and up to  $10^6$ ) and enhanced fluid fluxes during hydrothermal circulation (Delacour et al., 2005, 2007, 2008b).

A 100 m thick detachment shear zone (DSZ) has been mapped at the crest of the southern wall of the massif and is composed of highly deformed serpentinized peridotites and metasomatic talc- and/or amphibole-rich rocks (Boschi et al., 2006; Karson et al., 2006) that are related to strain localization and focused fluid flow (Schroeder and John, 2004; Boschi et al., 2006). Pelagic limestones, chalks, and sedimentary breccias with basaltic and serpentinitic clasts cover the DSZ (Früh-Green et al., 2003; Kelley et al., 2005; Karson et al., 2006). This carbonate cap is believed to act as a barrier for heat and hydrothermal fluids produced by the Lost City Hydrothermal Field (Früh-Green et al., 2003; Kelley et al., 2005).

The Lost City Hydrothermal Field (LCHF) is located on a fault-bounded terrace near the top of the southern AM (Fig. 2a and b) and is composed of numerous carbonate–brucite chimneys that reach up to 60 m in height and vent low-temperature (40–90 °C), alkaline (pH 9–11) fluids (Kelley et al., 2001, 2005; Ludwig et al., 2006). The fluids are poor in silica, metals and  $\text{CO}_2$ , rich in  $\text{CH}_4$  (1–2 mmol/kg),  $\text{H}_2$  (up to 15 mmol/kg) and Ca, and have elevated concentrations of other low-molecular weight hydrocarbons (Kelley et al., 2005; Proskurowski et al., 2008). Lithospheric cooling and subsurface exothermic mineral–fluid reactions in the underlying mantle rocks have driven hydrothermal activity at this site for at least 30,000 years (Früh-Green et al., 2003), and recent U–Th analyses indicate that this is a minimum age (Ludwig et al., 2005, 2006).

### 3. SAMPLES AND METHODS

The samples analyzed in this study were collected by drilling at IODP Site U1309 at the central dome and by submersibles at the southern wall (Fig. 2b; Expedition Scientific Party, 2005a,b; Blackman et al., 2006). The southern wall of the Atlantis Massif was investigated and sampled during three cruises: in 2000 and 2003 with the *R/V Atlantis* (AT3-60 and AT7-34 expeditions) and in 2005 with the *R/V R.H. Brown*. Details on the submersible sampling and lithologies are presented in Boschi et al. (2006) and Karson et al. (2006).

#### 3.1. Analytical methods

##### 3.1.1. Carbon contents and isotope compositions

Determination of total inorganic carbon (TIC) contents, released as  $\text{CO}_2$  from carbonate phases, was carried out at the Geological Institute, ETH Zurich by coulometric titration (Coulometer UIC CM5012).  $\text{CO}_2$  was liberated and analyzed by reaction of HCl with 20–30 mg of bulk rock powder in glass capsules. Carbonate contents were calculated from measured TIC based on the assumption that only calcium carbonate ( $\text{CaCO}_3$ , either as aragonite or as calcite) is present (Ludwig et al., 2006). The detection limit based on repeated measurements of blanks is 3 ppm. Relative precision of carbon content for replicate measurements of low amounts of calcium carbonate standard (99.95%  $\text{CaCO}_3$ ) is  $\pm 2\%$  ( $n = 17$ ). Reproducibility of individual samples is within  $\pm 5\%$ , whereas uncertainty is higher in samples with less than 20 ppm.

Analyses of carbon contents and carbon isotope compositions were determined from bulk rock powders at the Stable Isotope Laboratory, Geological Institute, ETH Zurich (Tables 1 and 2). Total organic carbon (TOC) was obtained by dissolution of carbonate carbon through addition of 1 N HCl to ~5 g of bulk sample powder. After complete reaction, the residual powders were washed several times with distilled water to completely remove the acid (checked with pH paper) and then dried at 90–100 °C. Finally, the residues were ground again in an agate mortar to obtain a fine-grained and homogeneous powder. With this method, graphite may also be present as a component of TOC. To minimize contamination by atmospheric CO<sub>2</sub>, the samples were degassed in an oven at 100 °C one day to one week before analysis.

Initial analyses of total carbon (TC) and TOC in samples from the southern wall and central dome were carried out on 60–90 mg of bulk powder weighed into tin capsules (9 × 11 mm size) and combusted in a Carlo Erba elemental analyzer (NCS 2500, CE Instruments, Milan, Italy) interfaced in continuous flow mode to a GV-INSTRUMENTS OPTIMA mass spectrometer. Complete combustion and long-term stability was tested by systematically measuring small-sized standards and blanks between samples. A second series of samples from the southern wall and all samples from the central dome were re-analyzed on 20–30 mg of sample using a Thermo Flash-elemental analyzer interfaced in continuous flow mode to a THERMO Instruments MAT253 mass spectrometer. Cross-calibration and comparison of the results of the two systems show analytical consistency between the two machines. Even when 90 mg of sample were used, combustion of organic carbon was complete. The detection limit for a reproducible carbon isotope measurement on the Micromass system was about 3 µg and for the Thermo system is about 1 µg C. Reproducibility of carbon contents of individual samples was within 15–20% and the carbon isotope compositions reproduced better than ±0.5‰.

Although we are confident in our determinations of the isotopic compositions and in the quantification of TIC and TOC, we find some discrepancies in the quantification of TC. We attribute the variations between different aliquots to heterogeneity in carbon contents in the bulk rock powders used to determine TC contents. We explicitly find no indication for incomplete combustion. Tests on the basis of mass balance and isotopic compositions lead us to the conclusion that calculated TC contents, based on the measured TIC and TOC contents, are better indicators of total carbon contents. Plots of TIC contents versus  $\delta^{13}\text{C}_{\text{TC}}$  values (Figs. 3b and 5b) clearly show that the bulk rock carbon isotope compositions ( $\delta^{13}\text{C}_{\text{TC}}$ ) reflect a mix of marine carbonate, with variable  $\delta^{13}\text{C}$  values (up to approximately 3‰), and organic carbon with a relatively constant  $\delta^{13}\text{C}$  value of approximately –26‰. The range of inferred C-isotope compositions of the carbonate in the bulk samples lie within the range measured in the hydrothermal precipitates at Lost City (Kelley et al., 2005).

Carbon isotope values are reported as standard  $\delta$ -notation relative to the Vienna-Pee Dee Belemnite (V-PDB) standard. The system was calibrated using the international

standards NBS22 and ANU sucrose for carbon isotope compositions and verified by using a low carbon standard (0.141 wt%) distributed by Hekatech GmbH (Germany) for carbon content. Carbon contents of the samples were calculated based on the area of mass 44 peak and corrected for blank contribution from the tin capsules. Analytical reproducibility of replicate measurements of standards is  $\pm 0.2\text{‰}$  ( $1\sigma$ ,  $n = 138$ ).

### 3.1.2. Solvent extraction

Extraction of organic compounds was carried out on selected serpentinitized peridotites (Table 3) and olivine-rich samples at the Laboratoire de Géochimie Bioorganique, Institut de Chimie de Strasbourg (France). For each sample, the 2 cm outer edges were removed to avoid external and superficial organic contamination prior to crushing in a tungsten carbide mortar or agate mortar, which were previously washed with organic solvents. For extraction, a 1:1 mixture of pre-distilled dichloromethane and methanol was added to ~100 g of fine-grained powder. After 30 min in an ultrasonic bath at ambient temperature, the mixture was centrifuged and the solvents were evaporated under reduced pressure. The organic extracts were separated on silica gel column into saturated (elution with hexane), aromatic (elution with a 8:2 volume per volume (v/v) mixture of hexane/dichloromethane), and polar hydrocarbon fractions (elution with a 1:1 v/v mixture of methanol/dichloromethane). Our study concentrates on the saturated hydrocarbon fractions; concentrations of the other fractions proved too small for a detailed characterization.

GC analyses were carried out on an Agilent 6890 gas chromatograph equipped with an on-column injector, a FID detector and a HP-5 fused silica capillary column (30 m × 0.32 mm; 0.25 µm film thickness) with H<sub>2</sub> as carrier gas. The temperature program was 40–200 °C at 10 °C/min, 200–300 °C (4 °C/min) and isothermal at 300 °C for 30 min. GC-MS analyses were carried out on an Agilent 6890 gas chromatograph equipped with a HP5 capillary column (30 m × 0.25 mm; 0.25 µm film thickness) connected to an Agilent 5975 MSD operated in the electron impact (EI) mode with a scan range of 50–700 Da. Helium was used as carrier gas. The temperature program was set at: 40–200 °C (10 °C/min), 200–300 °C (4 °C/min), and isothermal at 300 °C for 30 min.

Compound-specific carbon isotope ratios were determined on the saturated hydrocarbon fractions at the Department of Environmental Sciences (ETH Zurich) with a gas chromatograph-isotope ratio monitoring mass spectrometer (GC-IRMS). Two instruments were used, a Thermo Delta V plus IRMS and a Thermo Delta plus XL with combustion interface and Thermo Trace GC with HP5 capillary column (30 m × 0.25 mm; 0.25 µm film thickness). Helium was used as carrier gas. The temperature program was 40 °C for 1 min, 10°C/min to 200 °C, 200 °C for 10 min, 4°C/min to 280 °C and isothermal at 280 °C for 30 min. Each saturated hydrocarbon fraction was measured three times and the reported values are an average of the three measurements and corrected to a set of internal *n*-alkane standards. Carbon isotope compositions of each hydrocarbon (*n*-alkanes and isoprenoids) were obtained

Table 1

Content and carbon isotope compositions in total carbon (TC), total organic carbon (TOC) and total inorganic carbon (TIC) of gabbroic and ultramafic rocks from the central dome (IODP Holes 1309B and 1309D)

Hole/Leg	Sample number	Depth (mbsf)	Type of rock	Alteration (%)	TC <sup>a</sup> (ppm)	TIC (ppm)	TOC (ppm)	% TIC	$\delta^{13}\text{C}$ WR TC (‰)	$\delta^{13}\text{C}$ WR TOC (‰)
304-1309D	1R-1 72–80 cm	21.22	Basalt–diabase	50	202	101	101	50	−18.0	−27.8
304-1309D	1R-3 4–8 cm	23.31	Talc–schist	100	335	130	205	39	−22.2	−27.9
304-1309D	17R-2 9–17 cm	99.89	Gabbro	40	199	121	78	61	−20.9	−28.7
304-1309D	27R-3 6–9 cm	155.14	Harzburgite	90	2569	2186	383	85	−5.8	−26.9
304-1309D	31R-2 19–30 cm	173.15	Harzburgite	90	2713	2481	232	91	−3.2	−27.0
304-1309D	42R-1 0–8 cm	224.30	Talc-rich harzburgite	90	1838	823	1015	45	−8.6	−28.3
304-1309D	51R-4 30–38 cm	270.98	Gabbro	10	1240	235	1005	19	−24.9	−28.4
304-1309D	58R-1 50–57 cm	300.90	Olivine-rich troctolite	70	219	98	121	45	−14.7	−27.7
304-1309D	60R-3 36–46 cm	313.19	Troctolite	50	468	269	199	57	−16.3	−27.6
304-1309D	64R-1 6–17 cm	329.26	Troctolite	50	710	338	372	48	−14.4	−27.8
304-1309D	65R-2 22–30 cm	335.72	Cr-rich harzburgite	55	536	331	205	62	−8.7	−27.3
304-1309D	70R-2 80–90 cm	360.49	Olivine gabbro–troctolite gabbro	30	380	195	185	51	−11.8	−28.2
304-1309D	71R-3 32–38 cm	365.68	Olivine gabbro–troctolite gabbro	40	137	47	90	34	−20.1	−28.9
305-1309D	83R-1 16–26 cm	415.16	Olivine gabbro–troctolite gabbro	5	249	173	76	69	−14.9	−26.7
305-1309D	83R-1 54–64 cm	415.54	Olivine gabbro–troctolite gabbro	50	903	418	485	46	−9.7	−27.9
305-1309D	84R-2 8–17 cm	420.96	Oxide gabbro–leucocratic alteration	60	866	483	383	56	−15.4	−28.2
305-1309D	91R-2 46–54 cm	455.34	Troctolite	20	462	366	96	79	−10.7	−28.7
305-1309D	91R-2 110–117 cm	455.98	Troctolite	5	179	72	107	40	−17.5	−28.6
305-1309D	100R-1 42–46 cm	497.02	Olivine-rich troctolite	10	412	152	260	37	−15.2	−27.7
305-1309D	111R-1 111–116 cm	550.51	Troctolite	10	522	295	227	57	−9.1	−27.5
305-1309D	111R-4 31–39 cm	553.88	Troctolite	20	285	182	103	64	−11.4	−27.7
305-1309D	115R-4 60–70 cm	573.34	Olivine gabbro–troctolite gabbro	40	433	348	85	80	−11.9	−28.4
305-1309D	116R-1 58–68 cm	573.98	Oxide gabbro–leucocratic alteration	50	3188	2590	598	81	−5.7	−28.3
305-1309D	126R-2 15–20 cm	623.00	Oxide gabbro–leucocratic alteration	30	997	434	563	44	−10.9	−28.2
305-1309D	130R-2 47–56 cm	642.52	Gabbro	30	1621	1037	584	64	−6.3	−28.4
305-1309D	136R-2 21–29 cm	670.97	Olivine gabbro–troctolite gabbro	20	492	199	293	40	−13.7	−27.7
305-1309D	136R-2 60–71 cm	671.36	Olivine gabbro–troctolite gabbro	20	1063	576	487	54	−10.7	−27.9
305-1309D	137R-1 85–91 cm	675.05	Oxide gabbro	40	344	96	248	28	−21.4	−27.6
305-1309D	158R-1 47–51 cm	770.67	Gabbro	30	1822	1490	332	82	−5.2	−27.9
305-1309D	169R-1 90–100 cm	823.90	Gabbro	5	275	191	84	69	−15.1	−27.9
305-1309D	189R-4 60–71 cm	923.64	Troctolite	3	235	139	96	59	−12.0	−27.9
305-1309D	194R-2 70–80 cm	939.58	Olivine gabbro–troctolite gabbro	1	360	260	100	72	−15.7	−27.1
305-1309D	221R-3 120–130 cm	1066.98	Olivine gabbro–troctolite gabbro	5	229	113	116	49	−15.8	−27.4
305-1309D	227R-3 37–42 cm	1095.30	Olivine-rich troctolite	20	304	153	151	50	−17.7	−27.7

305-1309D	227R-3 104-109 cm	1095.97	Olivine-rich troctolite	5	352	157	195	45	-12.9	-27.1
305-1309D	232R-1 20-31 cm	1115.30	Olivine-rich troctolite	10	299	130	169	43	-11.5	-27.6
305-1309D	233R-1 24-30 cm	1120.14	Olivine gabbro-troctolite gabbro	30	471	175	296	37	-15.9	-27.4
305-1309D	234R-2 102-110 cm	1127.22	Olivine-rich troctolite	10	527	286	241	54	-12.5	-27.8
305-1309D	237R-2 7-17 cm	1140.59	Olivine-rich troctolite	10	450	242	208	54	-11.7	-27.9
305-1309D	241R-2 97-108 cm	1160.74	Olivine-rich troctolite	10	285	142	143	50	-11.5	-28.6
305-1309D	241R-2 117-123 cm	1160.94	Olivine gabbro-troctolite gabbro	30	167	74	93	44	-20.1	-27.7
305-1309D	248R-1 114-120 cm	1193.04	Olivine-rich troctolite	5	152	99	53	65	-15.4	-28.8
305-1309D	256R-2 46-56 cm	1231.90	Olivine-rich troctolite	10	656	404	252	62	-11.4	-27.4
305-1309D	292R-2 78-88 cm	1398.63	Gabbro	20	267	207	60	78	-17.3	-26.7
304-1309B	11R-1 23-30 cm	57.23	Harzburgite	90	573	417	156	73	-9.4	-28.2

<sup>a</sup> TC content is the sum of the measured TOC and TIC contents (TC = TOC + TIC).

by integrating only the peak area of the compound without accounting for the large amounts of unresolved complex mixture present in all chromatograms. Analytical reproducibility of replicate measurements of standards was  $\pm 0.4\%$  ( $1\sigma$ ,  $n = 14$ ).

## 4. RESULTS

### 4.1. Carbon contents and isotope compositions

The gabbroic rocks and serpentinites of the central dome show a wide range of total carbon (TC) contents, ranging from 137 ppm to 0.32 wt%, and  $\delta^{13}\text{C}_{\text{TC}}$  values of  $-24.9\%$  to  $-3.2\%$  (Table 1 and Fig. 3a). Carbon isotope compositions of total organic carbon (TOC; i.e. residues after decarbonation) lie in a narrower range with more negative values, from  $-28.9\%$  to  $-26.7\%$  (Fig. 4c). The serpentinites with the highest TC contents and  $\delta^{13}\text{C}_{\text{TC}}$  values contain a high proportion of total inorganic carbon (TIC; Fig. 3b) and are associated with high degrees of alteration (Fig. 4a and d). However, one serpentinite sample (304-1309D-42R-1 0-8 cm) with a high TC content also has a high TOC content (Table 1 and Fig. 4b). Below 800 m depth, the TC and TOC contents are low ( $<0.065$  wt%) and broadly uniform (Fig. 4a and b); minor variations in TC contents of the olivine-rich troctolites correlate with the presence of local fault zones (e.g., at 1100 mbsf, Fig. 4a). The  $\delta^{13}\text{C}_{\text{TOC}}$  values show a narrow range of values downhole, within the range of values of marine dissolved organic carbon (Fig. 4c).

The majority of the samples from the southern wall have less than 0.1 wt% total carbon and  $\delta^{13}\text{C}_{\text{TC}}$  values ranging from  $-28.7\%$  to  $+2.3\%$  (Table 2 and Fig. 5a). Total inorganic carbon accounts for 10-98% of the total carbon and the serpentinites with high TIC contents have positive  $\delta^{13}\text{C}_{\text{TC}}$  values around seawater value (Table 2 and Fig. 5b).  $\delta^{13}\text{C}_{\text{TOC}}$  values vary from  $-28.9\%$  to  $-21.5\%$ , with an average of  $-25.9\%$ , and overlap the range of isotopic compositions of marine dissolved organic carbon (Druffel et al., 1992; Des Marais, 2001). The gabbros from the southern wall have uniform total carbon contents (Table 2 and Fig. 5a), whereas the serpentinites and some of the metasomatic fault rocks have variable TC concentrations (average 360 ppm) and isotopic compositions ( $-24.4\%$  to  $-1.0\%$ ). The TC and TOC compositional ranges are similar to those measured for the serpentinites and gabbroic rocks from the central dome and differences between the two areas reside in higher inorganic carbon contents at the southern wall.

### 4.2. Organic geochemistry

#### 4.2.1. Southern Atlantis Massif

Results of organic compound extractions and gas chromatograms of the saturated hydrocarbon fractions of the serpentinites are shown in Table 3 and Figs. 6 and 7. The total extractable organic carbon contents of the serpentinites (saturated + aromatic + polar fractions) range from 21 to 41 ppm and most of the serpentinites have trace amounts that could not be quantified (Table 3). The

Table 2

Content and carbon isotope compositions in total carbon (TC), total organic carbon (TOC) and total inorganic carbon (TIC) of serpentinites, metasomatic fault rocks and gabbros from the southern Atlantis Massif

Sample numbers	Depth (mbsl)	Latitude N	Longitude W	Type of rock	Description of the samples	TC <sup>a</sup> (ppm)	TIC (ppm)	TOC (ppm)	% TIC	$\delta^{13}\text{C}$ WR TC (‰)	$\delta^{13}\text{C}$ WR TOC (‰)
3863-1301	834	30°7.512'	42°7.410'	Serpentinite	Static serpentinization, oxidized and late carb/cc veins	249	76	173	31	-13.2	-26.4
3867-1621	759	30°7.482'	42°7.140'	Serpentinite	Static serpentinization, oxidized and late carb/cc veins	154	74	80	48	-17.7	-26.8
3867-1623	759	30°7.488'	42°7.140'	Serpentinite	Static serpentinization	175	60	115	34	-13.2	-25.8
3872-1136a	798	30°7.482'	42°7.134'	Serpentinite	Static serpentinization	197	90	107	46	-16.1	-26.4
3873-1300	950	30°7.338'	42°7.776'	Serpentinite	Crystal-plastic deformation-ribbon texture	673	509	164	76	-4.9	-26.2
3876-1310	774	30°7.656'	42°7.834'	Serpentinite	Static serpentinization-talc metasomatism	398	310	88	78	-1.9	-26.1
3877-1158	1115	30°7.026'	42°7.122'	Serpentinite	Local metasomatism	242	128	114	53	-8.3	-26.6
3877-1307	1017	30°7.218'	42°7.140'	Serpentinite	Crystal-plastic deformation-local metasomatism	651	527	124	81	-1.0	-26.5
3877-1406	908	30°7.320'	42°7.200'	Serpentinite	Static serpentinization, late carb/cc veins	309	195	114	63	-7.2	-25.3
3881-1119	860	30°7.404'	42°7.128'	Serpentinite	Static serpentinization	61	6	55	10	-22.1	-26.4
3881-1132A	822	30°7.422'	42°7.098'	Serpentinite	Ribbon texture	279	199	80	71	-3.6	-24.6
3639-1355	1295	30°7.153'	42°8.226'	Serpentinite	Static serpentinization and HT deformation of orthopyroxene		155	n.d.		-20.8	n.d.
3647-1416	1555	30°7.130'	42°4.132'	Serpentinite	Talc-chlorite vein	354	97	257	27	-23.0	-27.2
3651-1252	792	30°7.407'	42°6.968'	Serpentinite	Mesh to ribbon texture and HT deformation of orthopyroxene	482	90	392	19	-20.2	-26.6
H03-R2301	820	30°7.246'	42°7.109'	Serpentinite	Minor crystal-plastic deformation	297	143	154	48	-19.7	-26.8
H03-R2243	834	30°7.246'	42°7.113'	Serp. + cc veins	Static serpentinization-late carb/cc veins	1750	1260	490	72	-0.8	-25.3
3873-1245	956	30°7.356'	42°7.806'	Serp. + cc veins	Local cataclastic deformation	1306	1202	104	92	-0.1	-22.8
3638-1029	2526	30°5.430'	42°8.345'	Serp. + cc veins	Oxidized and late cc veins		13,550	n.d.	98	2.3	n.d.
3638-1134	2449	30°5.516'	42°8.433'	Serp. + cc veins	Ribbon texture	9010	8800	210	98	-0.5	-23.2
3639-1254S	1474	30°6.955'	42°8.406'	Serp. + cc veins	Ribbon texture, partially oxidized		838	n.d.		-5.0	n.d.
3646-1409	1790	30°5.665'	42°6.011'	Serp. + cc veins	Hourglass texture		4270	n.d.		-9.5	n.d.
3650-1146	3041	30°4.049'	42°9.642'	Serp. + cc veins	Mesh to ribbon texture-HT deformation of orthopyroxene	16,007	15,740	267	98	0.9	-21.5
3650-1436	2937	30°4.505'	42°9.606'	Serp. + cc veins	Ribbon texture	6510	6220	290	96	1.6	-22.1
3652-1203	834	30°7.603'	42°6.759'	Serp. + cc veins		3533	3200	333	91	0.1	-26.7
3863-1157	862	30°7.506'	42°7.410'	Amphi-rich rock	Static amphibole metasomatism	208	59	149	28	-21.5	-27.8
3877-1313	1009	30°7.224'	42°7.140'	Amphi-rich rock	Crystal-plastic deform.-amph. metasomatism	1020	900	120	88	-2.7	-28.9
3646-1205	2327	30°4.929'	42°6.029'	Amphi-rich rock			28	n.d.		-24.4	n.d.
3642-1309	1751	30°10.297'	42°6.994'	Talc/amphi.-rich rock			47	n.d.		-22.5	n.d.
3645-1159T	957	30°7.355'	42°7.826'	Talc/amphi.-rich rock			43	n.d.		-21.6	n.d.



Table 3

Compound-specific carbon isotope ratios for *n*-alkanes extracted from serpentinites from the southern part of the Atlantis Massif

	3863-1301	3867-1623	3873-1300	3877-1307	3881-1119	3651-1252
Total extracted organic carbon content (ppm)	21	33	n.d.	n.d.	41	n.d.
TOC content (ppm)	173	115	164	124	55	392
$\delta^{13}\text{C}_{\text{TOC}}(\text{‰})$	-26.4	-25.8	-26.2	-26.5	-26.4	-26.6
<i>n</i> -Alkanes						
C <sub>14</sub>	n.d.	-28.7	n.d.	n.d.	n.d.	n.d.
C <sub>15</sub>	-28.5	-29.5	n.d.	n.d.	-28.9	-29.5
C <sub>16</sub>	-28.9	-30.3	-31.9	-30.1	-29.8	-29.1
Norpristane	-28.6	-30.2	-29.9	-29.3	-29.8	-29.0
C <sub>17</sub>	-29.1	-30.4	-31.2	-33.5	-30.6	-29.9
Pristane	n.d. <sup>a</sup>	n.d. <sup>a</sup>	-30.3	-30.7	n.d. <sup>a</sup>	n.d. <sup>a</sup>
C <sub>18</sub>	-28.9	-29.6	-30.3	-31.2	-30.0	-29.2
Phytane	-29.0	-30.2	-30.0	-30.4	-30.5	-28.9
C <sub>19</sub>	-29.8	-29.4	-29.5	-29.5	-29.1	-29.3
C <sub>20</sub>	-29.5	-28.4	-29.1	-28.6	-27.9	-28.9
C <sub>21</sub>	-29.0	-28.7	-30.0	-29.2	-27.8	-28.5
C <sub>22</sub>	-28.7	-29.2	-28.4	-28.8	-28.6	-29.4
C <sub>23</sub>	-27.4	n.d.	-29.6	-29.8	-27.3	-27.8
C <sub>24</sub>	-27.5	n.d.	-30.9	-30.7	-27.7	-27.8
C <sub>25</sub>	-27.9	n.d.	-32.3	-30.7	-27.8	-27.8
C <sub>26</sub>	-27.4	n.d.	-32.9	-33.6	-27.3	-27.2
Squalane	-26.1	n.d.	-30.3	-31.1	-27.5	-24.6
C <sub>27</sub>	n.d.	n.d.	-32.7	-33.7	-28.3	-28.3
C <sub>28</sub>	n.d.	n.d.	-35.4	-32.8	-28.2	-28.2
C <sub>29</sub>	n.d.	n.d.	-38.6	-34.3	n.d.	-27.2
C <sub>30</sub>	n.d.	n.d.	-29.7	-35.8	n.d.	-27.1

<sup>a</sup> Carbon isotope compositions of pristane from samples 3863-1301, 3867-1623, 3881-1119 and 3651-1252 could not be measured because of insufficient peak separation during the analysis.

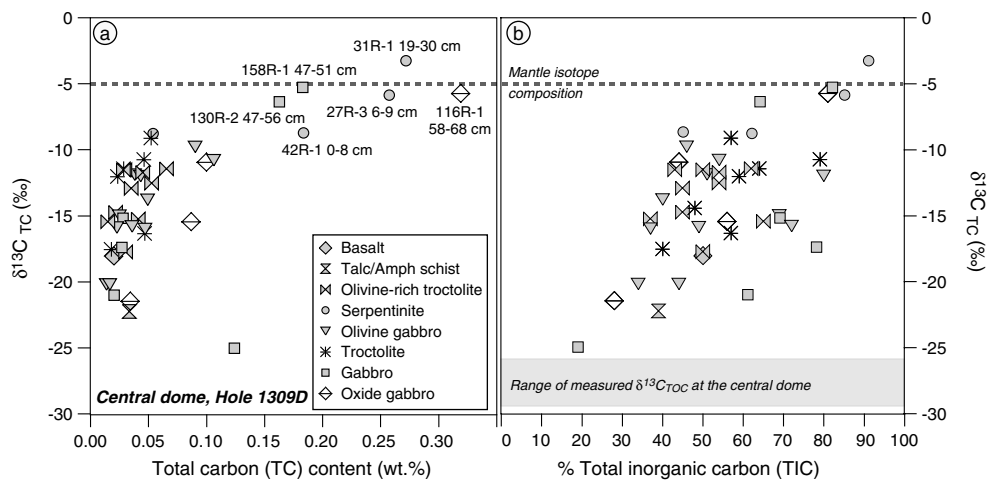


Fig. 3. (a)  $\delta^{13}\text{C}_{\text{TC}}$  values versus total carbon (TC) content of the gabbroic and ultramafic rocks at IODP Site U1309 at the central dome. The majority of the samples lie in a narrow range of isotopic composition from  $-24.9\text{‰}$  to  $-8.7\text{‰}$ . (b)  $\delta^{13}\text{C}_{\text{TC}}$  versus % total inorganic carbon (TIC) of the gabbroic and ultramafic rocks at the central dome showing that the bulk rock carbon isotope compositions ( $\delta^{13}\text{C}_{\text{TC}}$ ) reflect a mix of marine carbonate, with  $\delta^{13}\text{C}$  up to approximately  $3\text{‰}$ , and organic carbon with  $\delta^{13}\text{C}$  of approximately  $-26\text{‰}$ .

compound distribution with the serpentinites affected by the Lost City hydrothermal circulation. The troctolite 304-1309D-64R-1 6–17 cm, located at 329 mbsf, was chosen as representative of the top 800 m of the core where seawater alteration is more pronounced, and the olivine-rich troctolite 305-1309D-227R-3 6–12 cm, located at 1095 mbsf, is representative of the gabbroic and ultramafic rocks which are relatively unaffected by seawater circulation.

The total extracted organic carbon contents are  $\sim 5$  ppm and low compared to samples from the southern wall (Table 3). The saturated hydrocarbon fractions consist of *n*-alkanes ranging from C<sub>15</sub> up to C<sub>40</sub>. The gas chromatograms show a relatively homogeneous distribution, higher abundances of *n*-C<sub>16</sub> and *n*-C<sub>17</sub> alkanes and the presence of pristane, phytane and squalane. No odd over even carbon number predominance is observed; however the abun-

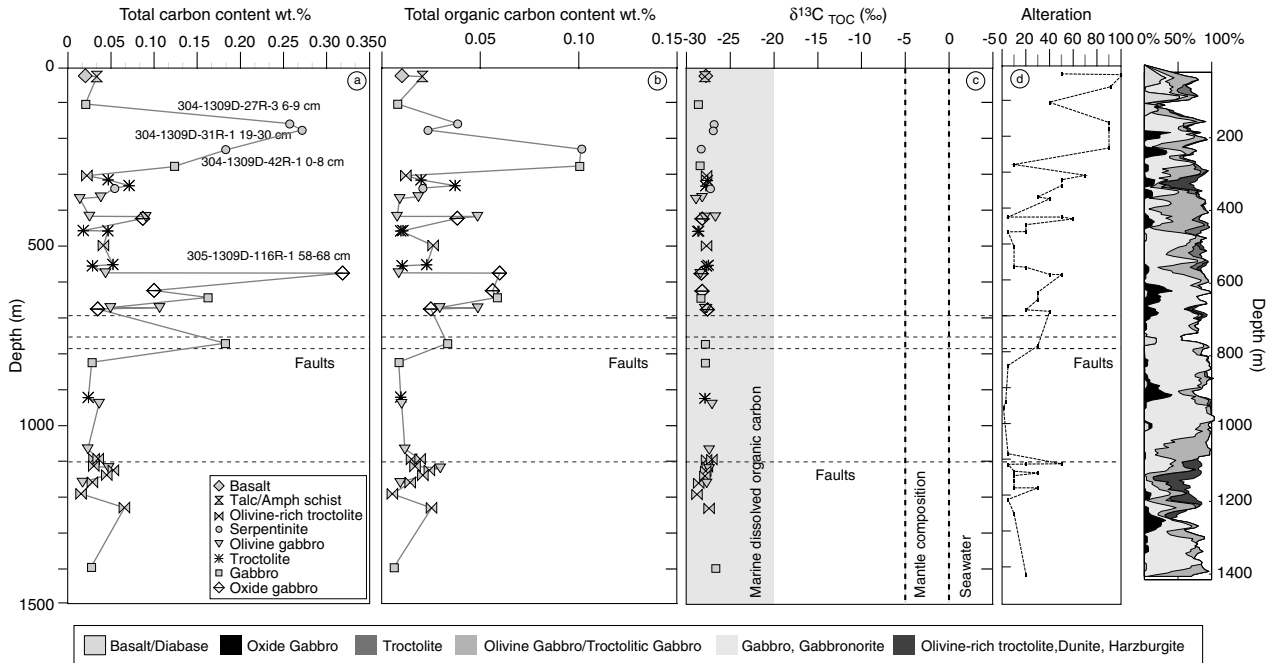


Fig. 4. Comparison of (a) total carbon (TC) content, (b) total organic carbon (TOC) content, (c)  $\delta^{13}\text{C}_{\text{TOC}}$ , and (d) alteration degree with depth and lithostratigraphy at Hole 1309D at the central dome of the Atlantis Massif. Depths of fault gouges identified by the IODP Shipboard Scientific Party are shown as horizontal dashed lines (695, 756, 785 and 1107 mbsf; Expedition Scientific Party, 2005a,b; Blackman et al., 2006). Serpentinized harzburgites from the upper 225 m are characterized by high TC contents. Below 800 m depth, the TC and TOC contents are broadly uniform, except some variations in the olivine-rich troctolites near the fault zone at 1100 mbsf. The  $\delta^{13}\text{C}_{\text{TOC}}$  values are uniform throughout the hole.

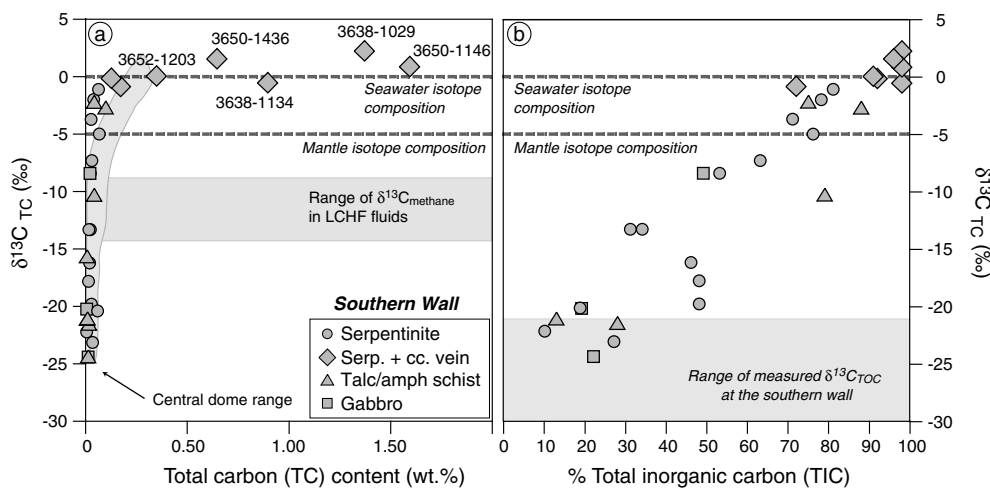


Fig. 5. (a) Variations in  $\delta^{13}\text{C}_{\text{TC}}$  values versus total carbon (TC) content of the serpentinites, metamorphic fault rocks and gabbros from the southern part of the Atlantis Massif. Positive  $\delta^{13}\text{C}_{\text{TC}}$  values correspond to serpentinites with calcite veins and indicate a marine carbon input. (b)  $\delta^{13}\text{C}_{\text{TC}}$  values versus % total inorganic carbon (TIC) showing that the bulk rock carbon isotope compositions ( $\delta^{13}\text{C}_{\text{TC}}$ ) reflect a mix of marine carbonate, with  $\delta^{13}\text{C}$  up to approximately 3‰, and organic carbon with  $\delta^{13}\text{C}$  of approximately  $-26$ ‰.

dances of the *n*-alkanes decrease with increasing carbon number (Fig. 9). Trace amounts of hopanes and steranes were also identified in these two samples. Compared to the gas chromatograms of the serpentinites from the southern wall, the distributions of hydrocarbons, such as the presence of longer-chained hydrocarbons, in the olivine-rich samples of the central dome are clearly different and may indicate different sources and processes of formation.

## 5. DISCUSSION

### 5.1. Origin of organic matter in the basement rocks

Five possible sources can be considered for the origin of organic compounds in the basement rocks of the Atlantis Massif and LCHF: (1) an abiotic origin through Fischer-Tropsch Type (FTT) reactions; (2) a biogenic origin

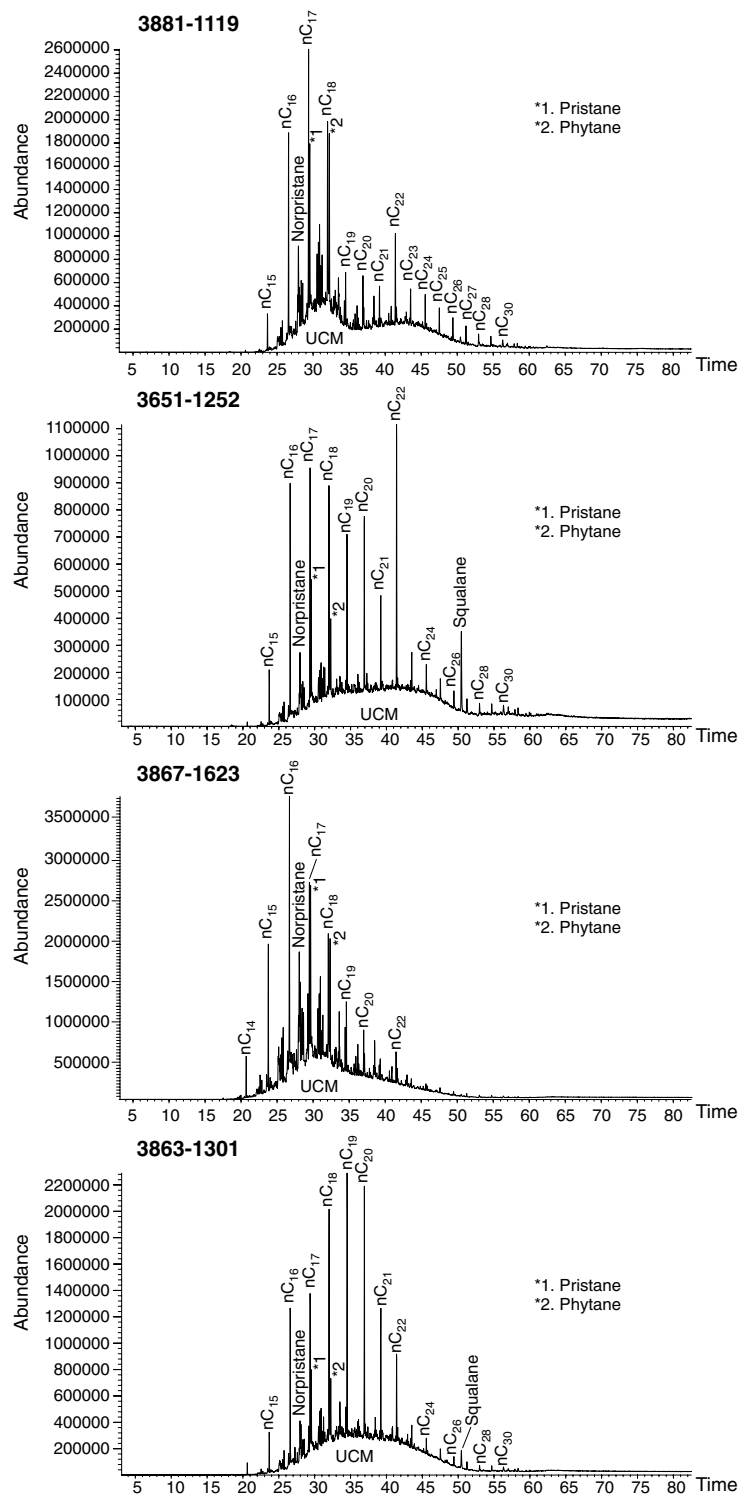


Fig. 6. Gas chromatograms showing the distributions of *n*-alkanes and isoprenoids (norpristane, pristane, phytane and squalane) in serpentinite samples 3881-1119, 3651-1252, 3867-1623, and 3863-1301. All chromatograms are distinct, which suggests that no contamination was recovered during the extraction procedure. The chromatograms exhibit higher abundances of C<sub>16</sub>–C<sub>20</sub> *n*-alkanes, which together with the isoprenoids suggest an input from marine dissolved organic carbon. The hump corresponds to the unresolved complex mixture (UCM) formed by branched and cyclic compounds. Sample 3651-1252, located at the basement of the Poseidon structure (Fig. 2b), shows the highest relative amounts of squalane, a potential biomarker for methane-cycling *Archaea*.

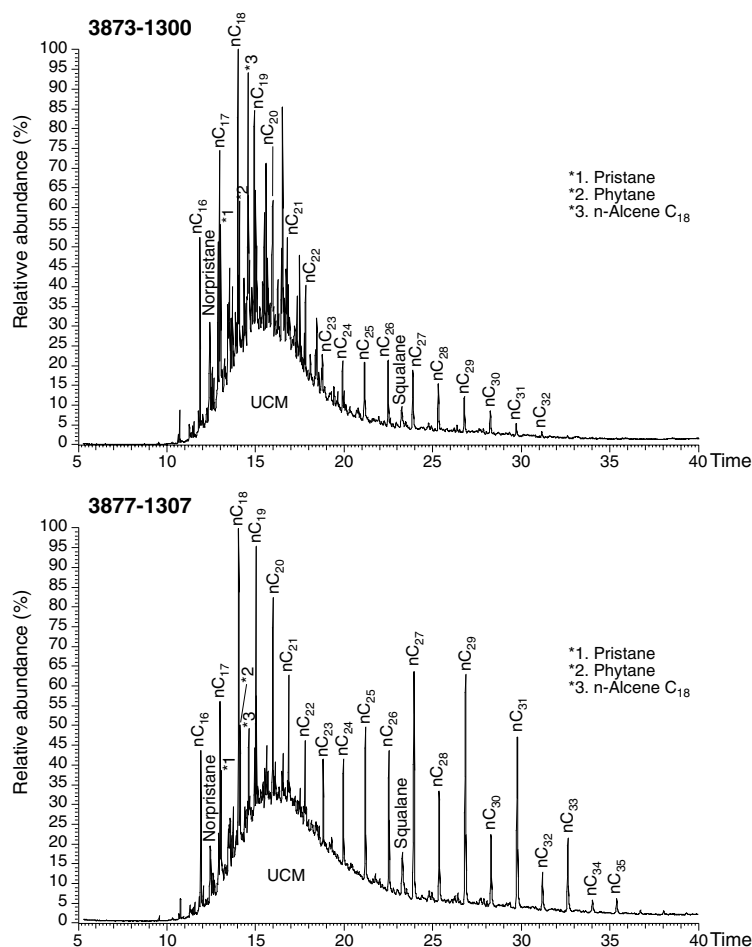


Fig. 7. Gas chromatograms showing the distributions of the *n*-alkanes and isoprenoids (norpristane, pristane, phytane and squalane) in serpentinite samples 3873-1300 and 3877-1307. Sample 3877-1307 is characterized by an odd over even carbon number predominance that reflects components of terrestrial plant waxes. Due to the location of the Atlantis Massif in the middle of the Atlantic, it is possible that this is related to settling of particulate organic matter or to contamination during sample handling.

through in-situ microbial activity in the basement rocks; (3) a thermogenic origin through thermal alteration of sedimentary organic matter; (4) an origin from incorporation of marine dissolved organic carbon (DOC) through seawater circulation; and (5) mantle carbon originating from organic matter present in sediments and recycled during subduction. Incorporation of particulate organic carbon (POC) through seawater circulation is not considered as a significant source of organic compounds in the basement rocks, as the pool of POC in deep seawater is relatively minor compared to DOC reservoir. In the following, we discuss first the evidence for a biological origin of organic matter at the Atlantis Massif and then possible contributions from abiotic reactions and other sources of hydrocarbons (recycling and thermogenic).

Companion studies of the Sr and Nd isotope geochemistry (Delacour et al., 2005, 2007, 2008b), the sulfide mineralogy, and sulfur geochemistry of the samples investigated here (Delacour et al., 2005, 2007) indicate that long-lived serpentinitization and alteration of the southern wall of the Atlantis Massif took place at distinctly high water–rock ratios (up to  $10^6$ ). North Atlantic deep ocean water contains

on average  $43 \mu\text{M}$  of DOC (Hansell and Carlson, 1998), thus, marine DOC transported into the basement rocks through extensive hydrothermal circulation must be considered as a viable source of carbon in the serpentinites.

The consistent presence of isoprenoids (pristane and phytane), the *n*-alkane distribution with chain lengths up to  $\text{C}_{40}$  maximizing between  $\text{C}_{16}$  and  $\text{C}_{20}$ , and the presence of hopanes and steranes in the basement rocks below Lost City point to a marine organic input of predominantly algal origin (Brassell et al., 1981; Mackenzie et al., 1982; ten Haven et al., 1988; Grice et al., 1998; de Leeuw et al., 1989; Kannenberg and Poralla, 1999; Volkman, 2006). Pristane and phytane are molecules originating from the phytol side-chain of chlorophyll-*a* in phototrophic organisms (Brassell et al., 1981) and were found in all of the serpentinites and olivine-rich troctolites. Phytane may also derive from lipids of some *Archaea*, notably those related to methane metabolism (Goossens et al., 1984; Volkman and Maxwell, 1986). Polycyclic compounds, hopanes and steranes, were identified in most of the serpentinites, with higher abundances found in samples close to the hydrothermal vents (3651-1252 and 3881-1119). Hopanes are common

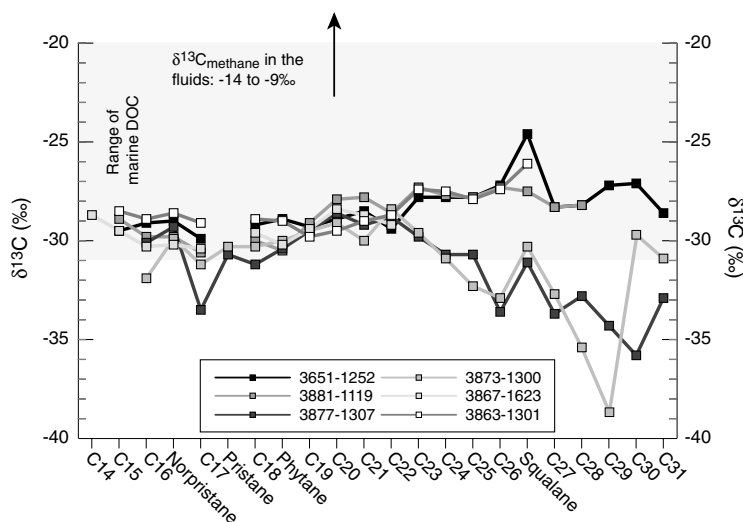


Fig. 8. Carbon isotope compositions of the *n*-alkanes and isoprenoids of the selected serpentinite samples from the southern Atlantis Massif. The samples show uniform carbon isotope compositions up to C<sub>22</sub>. For hydrocarbons >C<sub>22</sub>, two trends are visible, one grouping samples directly within the LCHF and another for samples located further away from the field (3877-1307 and 3873-1300). Peak C<sub>29</sub> of sample 3873-1300 is characterized by  $\delta^{13}\text{C}$  values of  $-38.6\text{‰}$ ; however, this value is likely insignificant due to the small size of the measured peaks.

components of cell membranes in eubacteria (Kannenberg and Poralla, 1999), whereas steranes are tetracyclic satu-

rated molecules derived from sterols, which are important components of membranes in marine or terrestrial eukary-

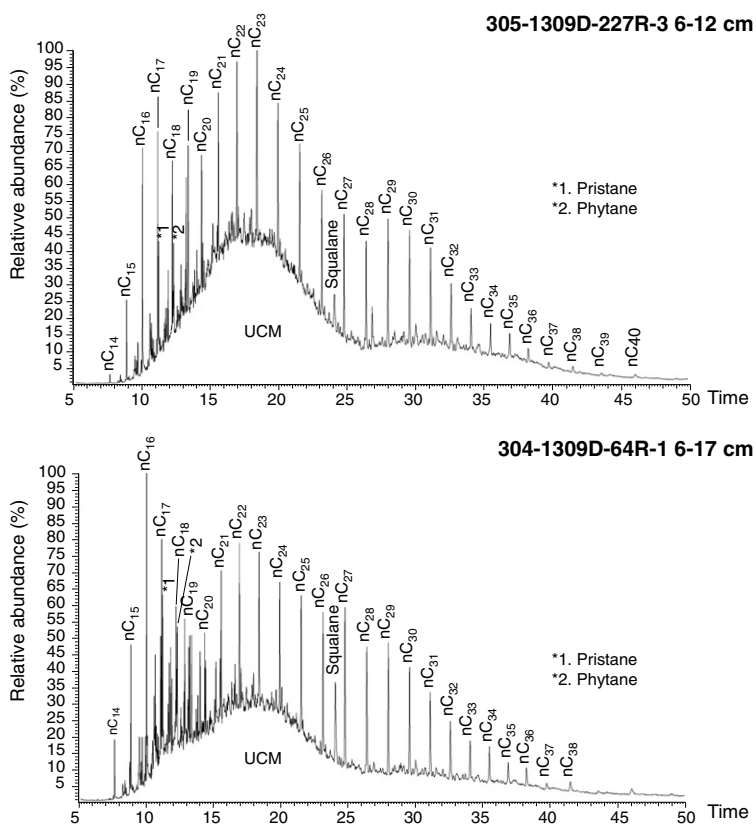


Fig. 9. Gas chromatograms showing the distributions of the *n*-alkanes and isoprenoids (norpristane, pristane, phytane and squalane) of two samples of the central dome: a troctolite 304-1309D-65R-2 6–17 cm and an olivine-rich troctolite 305-1309D-227R-3 6–12 cm. Both chromatograms show the presence of isoprenoids indicative of a marine carbon input, and suggest that seawater circulation through faults transported marine DOC at depth in the gabbroic section of the massif. The *n*-alkane distribution, characterized by a decrease in abundance with increasing carbon number, may also result from Fischer-Tropsch Type synthesis.

otic organisms (Mackenzie et al., 1982; de Leeuw et al., 1989; Volkman, 2006). Higher abundances of C<sub>16</sub> to C<sub>20</sub> *n*-alkanes characteristic of most of the samples at the southern wall (Figs. 6 and 7) are also consistent with a marine algal input (Volkman, 2006).

Squalane is an irregular acyclic isoprenoid. It is considered a biomarker for some *Archaea* (halophiles, methanogens or methanotrophs; Tornabene et al., 1979; Brassell et al., 1981; ten Haven et al., 1988; Grice et al., 1998; Brocks and Summons, 2003) and can be a component in marine DOC. The presence of squalane in the serpentinites may be attributed to methane-cycling *Archaea*, similar to those hosted in the carbonate chimneys and hydrothermal fluids of the LCHF (Lost City *Methanosarcinales* (LCMS) and ANME-1 phylotypes; Brazelton et al., 2006). The highest abundance of squalane was identified in sample 3651-1252 located directly beneath Poseidon (Fig. 2b). This active structure is characterized by high temperature (90 °C), high hydrogen content (Kelley et al., 2005; Proskurowski et al., 2006) and dense populations of microorganisms dominated by a single archaeal phylotype of LCMS (Brazelton et al., 2006).

A clear link between the presence of squalane and methane-cycling *Archaea* and hydrothermal activity at Lost City remains equivocal because squalane was detected in almost all serpentinite samples and was also found in the two olive-rich samples of the central dome. Squalane is synthesized by a wide range of organisms (Peters and Moldowan, 1993) and it (or its diagenetic transformation product squalane) may be an indicator of common marine microorganisms (e.g., algae). The presence of squalane together with other isoprenoids in the central dome samples may merely reflect incorporation of marine DOC during seawater alteration and imply that seawater circulated to a depth of 1095 mbsf at the central dome. However, isotopic studies of the central dome (Delacour et al., 2008a,b) indicate that seawater interaction is relatively limited at depth and circulation was mainly restricted to local fault zones. The presence of isoprenoids in the samples of the central dome cannot originate from contamination by the drilling mud and oil, which would be evidenced by higher abundances of long-chain hydrocarbons (C<sub>25</sub>–C<sub>40</sub>) and high-molecular weight cyclic compounds (Dunham, 2006). In addition, shipboard microbiological experiments with fluorescent microspheres was carried out to test potential contamination of the drilling fluid into the samples and revealed no contamination in the interior of the samples (Blackman et al., 2006).

Analyses of compound-specific carbon isotope compositions of the *n*-alkanes from the serpentinites of the southern wall yielded  $\delta^{13}\text{C}$  values from  $-38.6\text{‰}$  to  $-24.6\text{‰}$  (Table 3). These values are within the range of compositions of lipids derived from marine organic carbon, which are  $\sim 2\text{--}6\text{‰}$  lighter than the primary biomass ( $-18\text{‰}$  to  $-23\text{‰}$ ; Druffel et al., 1992; Hayes, 2001) and in the range of marine POC ( $\delta^{13}\text{C}$ :  $-30\text{‰}$  to  $-20\text{‰}$ ; Des Marais, 2001). The most negative  $\delta^{13}\text{C}$  values were found in samples 3877-1307 and 3873-1300 (Table 3), located furthest away from the active Lost City hydrothermal system and which show an odd over even carbon number predominance, typical of waxes

from C3 higher plants, and indicative of terrigenous inputs ( $\delta^{13}\text{C}$ :  $-36\text{‰}$  to  $-25\text{‰}$ ; Rieley et al., 1991, 1993). Similar occurrences were documented by Simoneit et al. (2004) for sulfide deposits of the Rainbow hydrothermal field, who point out the unlikelihood of transporting high-molecular weight odd *n*-alkanes from terrestrial higher plants to the mid-ocean ridges. Such an unexpected contribution of relatively recent biogenic material in the Lost City serpentinites could be attributed either to settling of particulate organic matter that has “contaminated” the rocks exposed at the seafloor, or to recent organic matter introduced during sample handling and preparation; however, we consider these possibilities to be very unlikely as all samples show different chromatograms. Variations in the  $\delta^{13}\text{C}$  values of pristane, phytane and squalane may reflect different metabolic pathways used by bacteria and/or *Archaea* for their synthesis (Hayes, 1993; Schouten et al., 1998). For example, Hayes (1993) reported differences of about 1.5‰ between the isoprenoids and the linear compounds synthesized from the same (micro)-organism. Schouten et al. (1998) show that phytol in algae is enriched in  $^{13}\text{C}$  of about 2–5‰ compared to the C<sub>16</sub> fatty acids due to their synthesis by two different metabolic pathways.

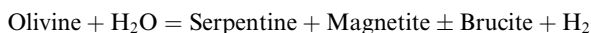
The carbon isotope compositions of the *n*-alkanes show a similar range of values as the  $\delta^{13}\text{C}_{\text{TOC}}$  of the serpentinites ( $-27.2\text{‰}$  to  $-21.5\text{‰}$ ), and for some samples, extracted organic fraction accounts for a significant proportion of the TOC content. Marine DOC transported by seawater into the serpentinites may likely be adsorbed on newly formed mineral surfaces. The efficiency of DOC sorption on surface minerals in sediments depends on a number of factors, such as temperature, redox conditions, pH, and water–rock ratios (Montluçon and Lee, 2001; Schwarzenbach et al., 2003; Svensson et al., 2004). Sorption decreases at elevated temperatures and reducing conditions (Montluçon and Lee, 2001; Svensson et al., 2004). The basement rocks of the LCHF are characterized by high fluid fluxes, oxidizing and moderate temperature conditions (Delacour et al., 2005, 2007, 2008b; Boschi et al., 2008) that will favor sorption of DOC in minerals. In addition, the serpentinites are mainly composed of phyllosilicate minerals (i.e. serpentine and chlorite) that favor uptake of organic molecules (Hedges, 1977; Wang and Lee, 1993).

## 5.2. Fischer-Tropsch Type (FTT) reactions and volatiles at the LCHF

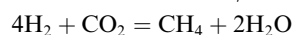
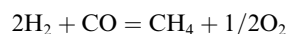
Despite evidence for a significant biogenic carbon component discussed above, we cannot a priori disregard the presence of an abiogenic contribution of hydrocarbons formed via Fischer-Tropsch Type (FTT) synthesis in the serpentinites. CH<sub>4</sub> and H<sub>2</sub> are significant components of the Lost City fluids, and carbon and hydrogen isotope studies indicate a dominant abiogenic origin (Kelley et al., 2005; Proskurowski et al., 2006, 2008). In addition, Proskurowski et al. (2008) reported low-molecular weight hydrocarbons (ethane, propane, butane) in the hydrothermal fluids and attribute these to an abiogenic carbon source from the basement rocks.

Abiotic formation of CH<sub>4</sub> and higher hydrocarbons via FTT has been investigated experimentally (Berndt et al.,

1996; Horita and Berndt, 1999; McCollom and Seewald, 2001, 2006, 2007) and is considered to be the primary mechanism for the origin of CH<sub>4</sub> in the ultramafic-hosted Rainbow hydrothermal fluids (Charlou et al., 1998; Holm and Charlou, 2001; Charlou et al., 2002; Douville et al., 2002; Simoneit et al., 2004). Serpentinization results in strongly reducing conditions through the reaction of ferrous iron-bearing minerals (i.e. olivine or orthopyroxene) with water and produces molecular H<sub>2</sub>. Hydrogen production will be limited by the amount of Fe oxidized and is generally described by the reaction:



Hydrogen may react with C-bearing species in the fluids, such as CO, CO<sub>2</sub>, or HCO<sub>3</sub><sup>-</sup> to produce CH<sub>4</sub> (Berndt et al., 1996; Horita and Berndt, 1999) and other long-chained hydrocarbons (McCollom and Seewald, 2006), via FTT reactions. FTT reactions commonly refer to industrial reduction of CO and include reactions, such as:



FTT reactions are enhanced by the presence of catalysts, such as iron- (e.g., magnetite) or nickel- and chromium-bearing minerals (Berndt et al., 1996; Foustoukos and Seyfried, 2004). In addition, a recent study of Fiebig et al. (2007) on low-temperature fumarolic gases of three Mediterranean volcanic systems indicated that hydrothermal reduction of CO<sub>2</sub> to CH<sub>4</sub> is favored by the presence of a saturated water vapor phase in the system and that chemical and isotopic equilibrium between CO<sub>2</sub> and CH<sub>4</sub> may be attained at temperatures as low as ~260 °C.

Experimental studies of aqueous FTT synthesis during serpentinization document the formation of abiotic hydrocarbons. These are characterized by: *n*-alkanes up to C<sub>35</sub>; a lack of carbon number predominance; and a decrease in *n*-alkanes abundance with increasing carbon number (see Fig. 2 in McCollom and Seewald, 2006, 2007). The studies of McCollom and Seewald (2006) determined a carbon isotope fractionation factor of about 36‰ between dissolved CO<sub>2</sub> and hydrocarbons, and showed that abiotic FTT synthesis can produce *n*-alkanes with δ<sup>13</sup>C values in the same range as those formed by biological processes. In these experimental studies, the longer-chain hydrocarbons were characterized by uniform and constant δ<sup>13</sup>C values indicating that no fractionation takes place during the polymerization step of FTT; however, ethane, propane and butane were <sup>13</sup>C-enriched relative to other hydrocarbons.

The distribution of *n*-alkanes in the olivine-rich samples of the central dome are characterized by a lack of odd over even carbon number predominance and a decrease in abundances of *n*-alkanes with increasing carbon number (Fig. 9) and, thus are comparable to the distribution found in FTT experiments. In contrast, the Lost City serpentinites show a distribution of hydrocarbons (Figs. 6 and 7) that are inconsistent with experimental results, suggesting a minimal contribution of *n*-alkanes by FTT. In addition, isoprenoids or other branched hydrocarbons have yet to be synthesized

in FTT experiments and no other abiotic sources of these compounds are known. Therefore, at present we can only attribute the presence of isoprenoids in the serpentinites and olivine-rich samples to a biologic origin.

Carbon for abiotic formation of hydrocarbons in the AM serpentinites has multiple possible sources: mantle CO<sub>2</sub>, dissolved seawater bicarbonate (HCO<sub>3</sub><sup>-</sup>), and/or acetate (CH<sub>3</sub>COO<sup>-</sup>) and formate (HCOO<sup>-</sup>) that may form during incipient serpentinization (McCollom and Seewald, 2001, 2003a,b). In a recent isotopic study, Proskurowski et al. (2008) argue that the source of carbon of the CH<sub>4</sub> and short-chained hydrocarbons in the hydrothermal fluids is mantle carbon rather than seawater bicarbonate. The carbon isotope compositions (-9‰ to -16‰) of the C<sub>1</sub>-C<sub>4</sub> hydrocarbons from the LCHF fluids are progressively negative with increasing chain length and are opposite to patterns for hydrocarbons produced thermogenically (Proskurowski et al., 2008). Therefore, a mantle source for potential abiotic formation of hydrocarbons in the basement rocks needs also to be considered, and their isotopic signatures may provide further constraints on processes of formation.

Reduction of CO<sub>2</sub> to formate or acetate during serpentinization produces negligible carbon isotope fractionation (Rishavy and Cleland, 1999) and their δ<sup>13</sup>C values will be similar to those of the mantle carbon source (~-5‰ to -7‰). Experimental studies indicate that abiotic formation of hydrocarbons from CO<sub>2</sub>, formate or acetate lead to δ<sup>13</sup>C values between -41‰ and -36‰ (McCollom and Seewald, 2006). Assuming a carbon isotope fractionation factor of 36‰ as proposed by McCollom and Seewald (2006), which does not change with reaction progress, abiotic synthesis of organic compounds in the serpentinites of the southern wall would require a carbon source with a positive δ<sup>13</sup>C value of about +2.5–+9‰. Carbon isotope analysis of carbonate from the Lost City towers indicate the presence of a heavy inorganic carbon component of up to at least +13‰ in the carbonate structures (Kelley et al., 2005); however, the source of the <sup>13</sup>C-enriched carbon remains equivocal. In addition, heavy isotopic compositions compared to background seawater DOC were also reported for excess DOC measured in the vent fluids (Lang et al., 2005).

While consistent with other C-isotope data from the LCHF, the compound-specific isotope signatures alone do not allow a clear verification nor quantification of contribution from abiotic mantle source. This discrepancy may not be surprising considering the fact that the samples collected by dredging or submersibles for our studies represent the “outer skin” of this system and, thus, the end-product of long-lived tectonic and hydrothermal activity during formation and emplacement of the massif as an OCC. Therefore, the chemical signatures used to infer sources and fluid fluxes may not be fully representative of the present-day conditions in the basement peridotites that directly feed the Lost City system. It is likely that marine organic compounds now dominate the carbon geochemistry of the samples investigated here, and the high seawater fluxes in the outermost wall of the massif have overprinted abiotic signatures of early stages of serpentinization and lower fluid fluxes.

### 5.3. Hydrocarbons in the oceanic lithosphere

There are few studies characterizing the carbon geochemistry and isotope compositions in mafic and ultramafic rocks, and the origin of  $^{13}\text{C}$ -depleted carbon components in the mantle remains controversial. Some authors suggest that carbon components extracted at low-temperature by step-heating experiments of basaltic and mantle rocks and characterized by  $\delta^{13}\text{C}$  values of  $-22\text{‰}$  to  $-26\text{‰}$  (Pineau and Javoy, 1983; Mathez, 1987; Deines, 2002) are due to organic contamination (Matthey et al., 1984). Other studies propose an indigenous origin of hydrocarbons with similar C-isotope compositions (Pineau and Mathez, 1990; Deines, 2002). Sugisaki and Mimura (1994) reported the presence of hydrocarbons ( $\text{C}_{14}$  to  $\text{C}_{33}$ ) in unaltered peridotites in ophiolites and in xenoliths, whereas these were lacking in their investigated serpentinite samples. Although a specific origin of the mantle hydrocarbons (biotic versus abiotic) was not clearly specified in the study of Sugisaki and Mimura (1994) they imply that hydrocarbons and isoprenoids (pristane and phytane) may be related to recycling of sediment material, rich in organic molecules, into the mantle. However, the absence of hydrocarbons in the serpentinites analyzed in the study of Sugisaki and Mimura (1994) contrasts with our results and with previous analyses of Früh-Green et al. (2004) on total organic carbon contents of serpentinites from various tectonic environments. Früh-Green et al. (2004) showed that up to 1500 ppm non-carbonate carbon may be trapped in oceanic serpentinites and conclude that a significant amount of this carbon may be present as hydrocarbons.

Our results from the southern wall of the AM provide new evidence for the presence of hydrocarbons in serpentinites. In particular, the *n*-alkanes in the serpentinites of the southern wall show no carbon number predominance and no decrease in abundance with increasing carbon number,

and are characterized by higher abundances in  $\text{C}_{16}$  to  $\text{C}_{20}$  *n*-alkanes and by the presence of isoprenoids; all of which strongly point to a marine source. In light of the high seawater fluxes recorded in the samples of the southern wall, we propose that organic carbon was introduced into the serpentinites from marine DOC during the long-lived history of water–rock interaction at the Atlantis Massif. The fact that the basement rocks, hydrothermal deposits and vent fluids at Lost City show marked variations in chemical and isotopic signatures suggests that different areas with varying degrees of serpentinization are presently being tapped by the seawater-derived fluids channeled and expelled along fault zones at the southern wall. At the central dome, there may be a contribution of *n*-alkanes by FTT reactions; however, the presence of pristane, phytane, squalane and higher abundances of *n*- $\text{C}_{16}$  and *n*- $\text{C}_{17}$  alkanes, together with the contribution of hopanes and steranes, point to a marine DOC input. Thus, relatively limited seawater circulation channeled in fault zones also seems to be capable of transporting small amounts of marine DOC deep in the gabbroic section of the central dome.

TOC contents and isotopic compositions of serpentinites and gabbros reported for other oceanic sites (e.g., Hess Deep, MARK, SWIR, Cayman Rise, Iberian Margin, Vema FZ, Mariana and Tyrrhenian Sea; Früh-Green et al., 1996; Kelley and Früh-Green, 1999, 2000, 2001; Früh-Green et al., 2004) are compared with the serpentinites and gabbros of the Atlantis Massif in Fig. 10. A wide range of  $\delta^{13}\text{C}$  values ( $-32\text{‰}$  to  $-16\text{‰}$ ) and TOC contents (20–1005 ppm) characterize the oceanic gabbros from the different localities. Within an individual site (Fig. 10a), TOC contents and carbon isotope compositions are variable and likely reflect the rock type or late fluid circulation during deformation and alteration. For example, the plutonic section of Hole 735B (SWIR) experienced a complex history of intrusion, deformation and penetration of

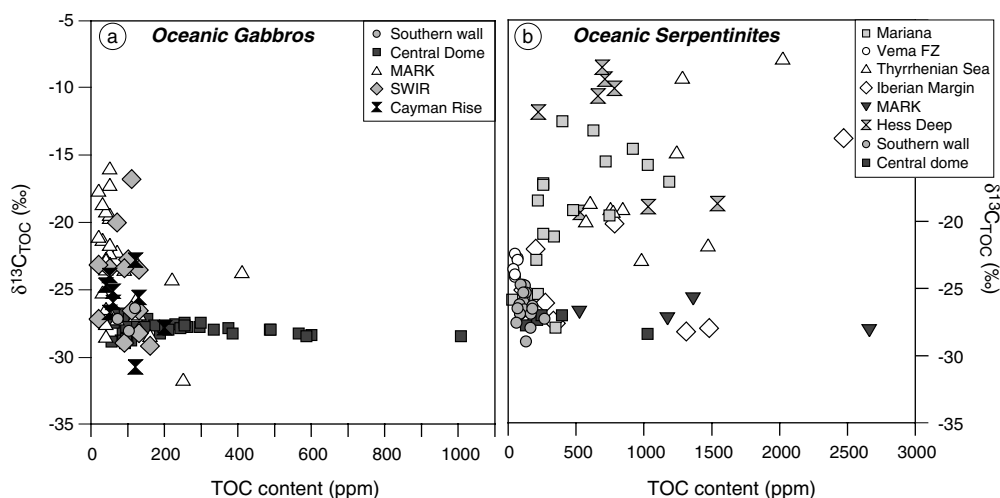


Fig. 10. Variations in  $\delta^{13}\text{C}_{\text{TOC}}$  versus total organic carbon (TOC) content of (a) oceanic gabbros and (b) oceanic serpentinites from various oceanic sites (Hess Deep, SWIR, MARK, Iberian Margin, Tyrrhenian Sea, Vema FZ; data from Früh-Green et al., 2004) compared with the basement rocks of the Atlantis Massif (central dome and southern wall). Oceanic serpentinites are characterized by high variations in carbon content and  $\delta^{13}\text{C}$  values, which likely reflect variations in serpentinization/alteration conditions and fluid fluxes, whereas oceanic gabbros show similar carbon contents and  $\delta^{13}\text{C}$  values, except some samples of the central dome showing higher TOC contents up to 1005 ppm.

hydrothermal fluids (Kelley and Fröh-Green, 1999), and the gabbroic rocks of Hess Deep re-equilibrated with late volatile-rich fluids (Kelley and Fröh-Green, 2000). The gabbroic rocks of the Atlantis Massif have carbon isotope compositions ( $-28.9\text{‰}$  to  $-26.6\text{‰}$ ) and TOC contents (Fig. 10a) within the range defined by the oceanic gabbros from various sites; however, some gabbros show high TOC contents (up to 1005 ppm; Fig. 10a).

Oceanic serpentinites from various settings also show a wide range of carbon isotope compositions ( $-28.9\text{‰}$  to  $-7.9\text{‰}$ ) and scattered TOC contents (20–2660 ppm; Fig. 10b). The majority of the serpentinites of the Atlantis Massif contain low TOC ( $<500$  ppm) and  $\delta^{13}\text{C}$  values that cluster in a narrow range between  $-30\text{‰}$  and  $-20\text{‰}$  (Fig. 10b). The low TOC contents and negative  $\delta^{13}\text{C}$  values may be related to low-temperature ( $<200$  °C) and more oxidizing alteration conditions (Delacour et al., 2005), as suggested by Fröh-Green et al. (2004) for the serpentinites from the Vema Fracture Zone and the Iberian Margin. Therefore, variations in total organic carbon contents and isotopic compositions of oceanic serpentinites may be related to variable carbon contents and speciation in the mantle, and the subsequent serpentinization conditions and fluid fluxes.

These compilations for oceanic serpentinites and gabbros (Fig. 10a and b) emphasize the heterogeneous carbon compositions of the oceanic crust (Kelley and Fröh-Green, 2000, 2001) and indicate that TOC in oceanic basement rocks are commonly characterized by depleted carbon isotope compositions. These signatures may be related either to the presence of organic compounds in the rocks (indigenous or transported) as documented in the Lost City serpentinites or to the presence of carbon volatiles ( $\text{CO}_2$ ,  $\text{CH}_4$ ) trapped in fluid inclusions. Kelley and Fröh-Green (1999, 2000, 2001) reported carbon isotope compositions for several generations of fluid inclusions trapped in the SWIR gabbroic rocks during a complex history of fluid speciation and alteration. The two main types,  $\text{CO}_2$ – $\text{CH}_4$ – $\text{H}_2\text{O}$ -bearing fluid inclusions and  $\text{CH}_4$ – $\text{H}_2$ -bearing fluid inclusions were analyzed for carbon isotope compositions. Both  $\text{CO}_2$  and  $\text{CH}_4$  show depleted isotopic compositions, with  $\delta^{13}\text{C}(\text{CO}_2)$  ranging from  $-24.9\text{‰}$  to  $-1.9\text{‰}$  and  $\delta^{13}\text{C}(\text{CH}_4)$  ranging from  $-27.1 \pm 4.3\text{‰}$  (Kelley and Fröh-Green, 2001). The occurrences of similar volatile phases in fluid inclusions have been reported from other areas, e.g., MARK and Hess Deep (Kelley, 1996, 1997; Kelley and Malpas, 1996). These volatiles may be more widespread than previously realized and may account for a significant contribution to the depleted carbon isotope signature of plutonic and ultramafic rocks in the oceanic crust.

## 6. CONCLUSIONS

This study contributes new data on the geochemistry of organic carbon in oceanic serpentinites and gabbroic rocks and provides constraints on the fate of dissolved organic carbon in seawater during long-lived serpentinization and hydrothermal alteration of the oceanic lithosphere. The occurrences of isoprenoids (pristane, phytane and squalane), polycyclic compounds (hopanes and steranes) and

higher abundances of  $n\text{-C}_{16}$  to  $n\text{-C}_{20}$  alkanes in the serpentinites of the southern wall point to a marine organic input with a possible minor component from in-situ chemosynthesis indicated by the high content of squalane in a serpentinite sample forming the basement of the active hydrothermal chimney Poseidon. In contrast, FTT reactions have been invoked to explain the origin of  $\text{C}_1$  to  $\text{C}_4$  hydrocarbons and a  $^{13}\text{C}$ -enriched excess of DOC in the hydrothermal vent fluids at Lost City (Lang et al., 2005; Proskurowski et al., 2008). Although an abiogenic formation of  $n$ -alkanes is also consistent with the presence of methane and hydrogen in the vent fluids, there is no clear evidence for a significant inorganic source of  $n$ -alkanes in the serpentinites of the southern wall. We propose that the high seawater fluxes in the basement rocks of the southern part of the AM likely favor the transport of marine DOC into the serpentinites and overprint any earlier abiotic signature acquired during initial stages of serpentinization and lower fluid fluxes. Thus, our study suggests that hydrocarbons account for an important proportion of the total carbon stored in the Atlantis Massif serpentinites and that serpentinites may represent an important—as yet unidentified—reservoir of DOC from seawater.

The detection of the biomarkers pristane, phytane and squalane at depths of 1095 mbsf at the central dome further implies seawater circulation deep into the gabbroic rocks likely using fault zones as pathways. However, the distribution of the  $n$ -alkanes characterized by a decrease in abundance with increase in carbon number may be attributed to formation by FTT synthesis. Unfortunately, the low concentrations of the saturated fractions in these samples precluded compound-specific isotopic characterization.

Hansell and Carlson (1998) reported a decrease in DOC concentration of  $\sim 14$   $\mu\text{M}$  of deep water between the North Atlantic and the North Pacific oceans, but the mechanisms of this removal are not well understood (Hansell, 2002). Circulation of deep water DOC through the oceanic crust may affect the oceanic DOC reservoir. Lang et al. (2006) calculated a global loss of 0.7 to  $1.4 \times 10^{10}$  g C/yr through high temperature axial vents, which accounts for less than 2% of the  $\sim 14$   $\mu\text{M}$  DOC loss during the oceanic deep circulation. High seawater fluxes, characteristic of the Lost City serpentinite-hosted hydrothermal system, and the sorption efficiency of newly formed phyllosilicates in serpentinite-dominated portions of oceanic crust may account for a relatively significant removal of DOC from the oceans to the oceanic crust. In addition, these data have to be considered into estimates of carbon fixed in the oceanic crust.

Assuming the extracted organic carbon fractions only originate from dissolved organic carbon in seawater, this extracted organic carbon content in the basement rocks of the Atlantis Massif, ranging from 5 to 41 ppm (Table 3), would give an estimation of the DOC trapped in the oceanic crust per year. Using the crustal production rate of  $6.0 \pm 0.8 \times 10^{16}$  g/yr calculated by Mottl (2003) and assuming that approximately 20–25% of the oceanic crust is composed of serpentinized peridotites (Cannat et al., 1995), so that only 5% of the new seafloor produced per year is composed of ultramafic rocks (Bach et al., 2001), this gives an estimate of the annual storage rate of organic carbon in

the oceanic crust ranging from  $1.5 \times 10^{10}$  to  $1.2 \times 10^{11}$  mol C/yr. In earlier studies, Staudigel et al. (1989) and Alt and Teagle (1999) estimated that the crust is a net sink of  $1.5\text{--}2.7 \times 10^{12}$  mol C/yr; however, this calculation accounts only for the inorganic carbon component (i.e. carbonate veins) and our studies indicates a further carbon component derived from DOC. Further investigations on oceanic serpentinites and gabbros may help to better constrain the amount of DOC removed through seawater circulation in the oceanic crust and consequently to better understand the carbon cycle.

Several authors (Shock, 1990; Holm et al., 1992, 2006; Shock and Schulte, 1998; Martin and Russel, 2006) propose that abiotic formation of organic compounds necessary for early life requires alkaline conditions and high  $\text{H}_2$  content in hydrothermal fluids. Similarly,  $\text{H}_2$ - and  $\text{CH}_4$ -rich and alkaline hydrothermal fluids produced by serpentinization of mantle peridotites typify the Lost City hydrothermal system and sustain dense microbial communities. Future studies of modern active peridotite-hosted hydrothermal systems and the linkages among serpentinization, volatiles and microbial activity may thus shed new light on the conditions of emergence of life on Earth.

#### ACKNOWLEDGMENTS

We thank the captains, crews, and technical staffs of *Alvin*, *Argo II*, and *ABE* aboard *R/V Atlantis* during cruises AT3-60 and AT7-34 to the Atlantis Massif in 2000 and 2003 for their support of this project. We also thank Jeffrey Karson, Donna Blackman, and the *Atlantis* and IODP co-chiefs and scientific parties for contributions to the data collection and discussions at sea. We also acknowledge Maria Coray-Strasser and Jakov Bolotin for assistance with the analyses. The authors appreciate the helpful comments of the three anonymous reviewers and associate editor Jeff Seewald. The NOAA Ocean Exploration Program to Lost City and Bob Ballard provided additional samples and images of key outcrops. This work was supported by ETH Grant 0-20890-01 to Früh-Green, Swiss SNF Grants 2100-068055 and 200020-107620 to Früh-Green and Bernasconi, and NSF Grant OCE-0426109 to Kelley.

#### REFERENCES

- Alt J. C. and Teagle D. A. H. (1999) The uptake of carbon during alteration of ocean crust. *Geochim. Cosmochim. Acta* **63**, 1527–1535.
- Bach W., Alt J. C., Niu Y., Humphris S., Erzinger J. and Dick H. J. B. (2001) The geochemical consequences of late-stage low-grade alteration of lower ocean crust at the SW Indian Ridge: results from ODP Hole 735B (Leg 176). *Geochim. Cosmochim. Acta* **65**, 3267–3287.
- Baross J. A. and Deming J. W. (1995) Growth at high temperatures: isolation and taxonomy, physiology, and ecology. In *The Microbiology Deep-Sea Hydrothermal Vents* (ed. D. M. Karl). CRC Press, pp. 169–217.
- Berndt M. E., Allen D. E. and Seyfried W. E. (1996) Reduction of  $\text{CO}_2$  during serpentinization of olivine at 300 °C and 500 bar. *Geology* **24**, 351–354.
- Blackman D. K., Cann J. R., Janssen B. and Smith D. K. (1998) Origin of extensional core complexes: evidences from the Mid-Atlantic Ridge at Atlantis Fracture Zone. *J. Geophys. Res.* **103**, 21315–21333.
- Blackman D. K., Karson J. A., Kelley D. S., Cann J. R., Früh-Green G., Gee J. S., Hurst S. D., John B. E., Morgan J., Nooner S. L., Kent Ross D., Schroeder T. J. and Williams E. A. (2002) Geology of the Atlantis Massif (Mid-Atlantic Ridge, 30°N): implications for the evolution of an ultramafic oceanic core complex. *Mar. Geophys. Res.* **23**, 443–469.
- Blackman D. K., Ildefonse B., John B. E., Ohara Y., Miller D. J., MacLeod C. J. and the Expedition 304/305 Scientists (2006) In *Proceedings Integrated Ocean Drilling Program, 304/305*. College Station TX (Integrated Ocean Drilling Program Management International, Inc.). doi:10.2204/iodp.proc.304305.2006.
- Boschi C., Früh-Green G. L., Delacour A., Karson J. A. and Kelley D. S. (2006) Mass transfer and fluid flow during detachment faulting and development of an oceanic core complex, Atlantis Massif (MAR 30°N). *Geochem. Geophys. Geosyst.* **7**, Q01004. doi:10.1029/2005GC001074.
- Boschi C., Dini A., Früh-Green G. L. and Kelley D. S. (2008) Isotopic and element exchange during serpentinization and metasomatism at the Atlantis Massif: insights from B and Sr isotopes. *Geochim. Cosmochim. Acta* **72**, 1801–1823. doi:10.1016/j.gca.2008.01.013.
- Bougault H., Charlou J.-L., Fouquet Y., Needham H. D., Vaslet N., Appriou P., Jean-Baptiste P., Rona P. A., Dmitriev L. and Silantiev S. (1993) Fast and slow spreading ridges: structures and hydrothermal activity, ultramafic topographic highs, and  $\text{CH}_4$  output. *J. Geophys. Res.* **98**, 9643–9651.
- Brassell S. C., Wardroper A. M. K., Thomson I. D., Maxwell J. R. and Eglinton T. I. (1981) Specific acyclic isoprenoids as biological markers of methanogenic bacteria in marine sediments. *Nature* **290**, 693–696.
- Brazelton W. J., Schrenk M. O., Kelley D. S. and Baross J. A. (2006) Methane- and sulfur-metabolizing microbial communities dominate the Lost City Hydrothermal Field ecosystem. *Appl. Environ. Microbiol.* **72**, 6257–6270.
- Brocks J. J. and Summons R. E. (2003) Sedimentary biomarkers, biomarkers for Early life. In *Treatise of Geochemistry*, vol. 8 (eds. H. Elderfield, H. D. Holland and K. K. Turekian), pp. 63–115.
- Cann J. R., Blackman D. K., Smith D. K., McAllister E., Janssen B., Mello S., Avgerinos E., Pascoe A. R. and Escartin J. (1997) Corrugated slip surfaces formed at ridge-transform intersections on the Mid-Atlantic Ridge. *Nature* **385**, 329–332.
- Cannat M., Mével C., Maia M., Deplus C., Durand C., Gente P., Agrinier P., Belarouchi A., Dubuisson G., Humler E. and Reynolds J. (1995) Thin crust, ultramafic exposures, and rugged fault patterns at the Mid-Atlantic Ridge (22°–24°N). *Geology* **23**, 49–52.
- Charlou J.-L. and Donval J.-P. (1993) Hydrothermal methane venting between 12°N and 26°N along the Mid-Atlantic Ridge. *J. Geophys. Res.* **98**, 9625–9642.
- Charlou J.-L., Bougault H., Appriou P., Nelsen T. and Rona P. A. (1991) Different TDM/ $\text{CH}_4$  hydrothermal plume signatures: TAG site at 26°N and serpentinized ultrabasic diapir at 15°05'N on the Mid-Atlantic Ridge. *Geochim. Cosmochim. Acta* **55**, 3209–3222.
- Charlou J. L., Fouquet Y., Bougault H., Donval J. P., Etoubleau J., Jean-Baptiste P., Dapoigny A., Appriou P. and Rona P. A. (1998) Intense  $\text{CH}_4$  plumes generated by serpentinization of ultramafic rocks at the intersection of the 15°20'N fracture zone and the Mid-Atlantic Ridge. *Geochim. Cosmochim. Acta* **62**, 2323–2333.
- Charlou J. L., Donval J. P., Fouquet Y., Jean-Baptiste P. and Holm N. (2002) Geochemistry of high  $\text{H}_2$  and  $\text{CH}_4$  vent fluids issuing from ultramafic rocks at the Rainbow hydrothermal field (36°14'N, MAR). *Chem. Geol.* **191**, 345–359.

- Deines P. (2002) The carbon isotope geochemistry of mantle xenoliths. *Earth Sci. Rev.* **58**, 247–278.
- Delacour A., Früh-Green G. L., Bernasconi S. M. and Kelley D. S. (2005) The influence of high seawater fluxes on sulfur compositions of the serpentinized peridotites at the Lost City Hydrothermal Field. *EOS Trans. AGU* **86**(52), Fall Meet. Suppl., Abstract V51B-1488.
- Delacour A., Früh-Green G. L. and Bernasconi S. M. (2006) Stable (C- and S-) isotope compositions of serpentinized ultramafics and gabbros from Hole 1309D on the Central Dome of the Atlantis Massif, 30°N MAR. *EuroForum*.
- Delacour A., Früh-Green G. L., Bernasconi S. M., Schaeffer P., Frank M., Gutjahr M. and Kelley D. S. (2007) Influence of high fluid fluxes on sulfur and carbon speciation of serpentinites of the Atlantis Massif. *Geophys. Res. Abstr.* **9**, 030907.
- Delacour A., Früh-Green G. L., Bernasconi S. M., Schaeffer P., Frank M. and Gutjahr M. (2008a) Isotopic constraints on seawater–rock interaction and redox conditions of the gabbro-dominated IODP Hole 1309D, Atlantis Massif (30°N, MAR). *Geophys. Res. Abstr.* **10**, EGU2008-A-08649.
- Delacour A., Früh-Green G. L., Frank M., Gutjahr M. and Kelley D. S. (2008b) Sr- and Nd-isotope geochemistry of the Atlantis Massif (30°N, MAR): implications for fluid fluxes and lithospheric heterogeneity. *Chem. Geol.*, in press. doi:10.1016/j.chemgeo.2008.05.018.
- Delaney J. R., Kelley D. S., Lilley M. D., Butterfield D. A., Barross J. A., Wilcock W. S. D., Embley R. W. and Summit M. (1998) The quantum event of oceanic crustal accretion: impacts of diking at mid-Ocean Ridges. *Science* **281**, 222–230.
- Deming J. W. and Baross J. A. (1993) Deep sea smokers—windows to a subsurface biosphere. *Geochim. Cosmochim. Acta* **57**, 3219–3230.
- Des Marais D. J. (2001) Isotopic evolution of the biogeochemical carbon cycle during the Precambrian. In *Stable Isotope Geochemistry*, vol. 43 (eds. J. W. Valley and D. R. Cole). Reviews in Mineralogy and Geochemistry, pp. 555–578.
- Donval J. P., Charlou J.-L., Douville E., Knoery E. and Fouquet Y. (1997) High H<sub>2</sub> and CH<sub>4</sub> content in hydrothermal fluids from Rainbow site newly samples at 36°14'N on the AMAR segment, Mid-Atlantic Ridge (diving FLORES cruise, July 1997). Comparisons with other MAR dives. *EOS Trans. AGU* **78**, 832.
- Douville E., Charlou J. L., Donval J. P., Knoery J. and Fouquet Y. (1997) Trace elements in fluids from the new Rainbow hydrothermal field (36°14' N, MAR): a comparison with other Mid-Atlantic Ridge fluids. *EOS Trans. AGU* **78**, 832.
- Douville E., Charlou J. L., Oelkers E. H., Bienvenu P., Jove Colon C. F., Donval J. P., Fouquet Y., Prieur D. and Appriou P. (2002) The Rainbow vent fluids (36°14'N, MAR): the influence of ultramafic rocks and phase separation on trace metal content in Mid-Atlantic Ridge hydrothermal fluids. *Chem. Geol.* **184**, 37–48.
- Druffel E. R. M., Williams P. M., Bauer J. E. and Ertel J. R. (1992) Cycling of dissolved and particulate organic-matter in the open ocean. *J. Geophys. Res.* **97**, 15639–15659.
- Dunham K. W. (2006) Potential organic geochemical contaminants on board the Joides Resolution. In *Proceedings of Ocean Drilling Program Initial Results*, vol. 103, pp. 71–74. doi:10.2973/odp.proc.ir.103.104.1987.
- Expedition Scientific Party (2005a) Oceanic core complex formation, Atlantis Massif, *IODP Prel. Rept.*, 304. Available from: <http://iodp.tamu.edu/publications/PR/304PR/304PR.PDF>.
- Expedition Scientific Party (2005b) Oceanic core complex formation, Atlantis Massif, *IODP Prel. Rept.*, 305. Available from: <http://iodp.tamu.edu/publications/PR/305PR/305PR.PDF>.
- Fiebig J., Woodland A. B., Spangenberg J. and Oschmann W. (2007) Natural evidence for rapid abiogenic hydrothermal generation of CH<sub>4</sub>. *Geochim. Cosmochim. Acta* **71**, 3028–3039.
- Fisher C. R. (1995) Toward an appreciation of hydrothermal-vent animals: their environment, physiological ecology, and tissue stable isotope values. In *Seafloor Hydrothermal Systems: Physical, Chemical, Biological, and Geological Interactions*, vol. 70 (eds. S. E. Humphris, R. A. Zierenberg, L. S. Mullineaux and R. E. Thomson). American Geophysical Union, Washington, DC, pp. 297–316.
- Fornari D. J. and Embley R. W. (1995) Tectonic and volcanic controls on hydrothermal processes at the mid-ocean ridge: an overview based on near-bottom and submersible studies. In *Seafloor Hydrothermal Systems: Physical, Chemical, Biological, and Geological Interactions*, vol. 70 (eds. S. E. Humphris, R. A. Zierenberg, L. S. Mullineaux and R. E. Thomson). American Geophysical Union, Washington, DC, pp. 1–46.
- Foustoukos D. I. and Seyfried W. E. J. (2004) Hydrocarbons in hydrothermal vent fluids: the role of chromium-bearing catalysts. *Science* **304**, 1002–1005.
- Früh-Green G. L., Plas A. and Lécuyer C. (1996) Petrologic and stable isotope constraints on hydrothermal alteration and serpentinization of the EPR shallow mantle at Hess Deep (Site 895). *Proc. Ocean Drill. Program, Sci. Results* **147**, 255–292.
- Früh-Green G. L., Kelley D. S., Bernasconi S. M., Karson J. A., Ludwig K. A., Butterfield D. A., Boschi C. and Proskurowski G. (2003) 30,000 Years of hydrothermal activity at the Lost City Vent Field. *Science* **301**, 495–498.
- Früh-Green G. L., Connolly J. A. D., Plas A., Kelley D. S. and Grobety B. (2004) Serpentinization of oceanic peridotites: implications for geochemical cycles and biological activity. In *The Subseafloor Biosphere at Mid-ocean Ridges*, vol. 144 (eds. W. S. D. Wilcock, E. F. DeLong, D. S. Kelley, J. A. Baross and S. C. Cary). American Geophysical Union, Washington, DC, pp. 119–136.
- German C. R. and Von Damm K. L. (2003) Hydrothermal processes. In *Treatise on Geochemistry*, vol. 6. (eds. H. Elderfield, H. D. Holland and K. K. Turekian), pp. 181–222.
- Goossens H., de Leeuw J. W., Schenck P. A. and Brassel S. C. (1984) Tocopherols as likely precursors of pristane in ancient sediments and crude oils. *Nature* **312**, 440–442.
- Gough M. A., Rhead M. M. and Rowland S. J. (1992) Biodegradation studies of unresolved complex mixtures of hydrocarbons: model UCM hydrocarbons and the aliphatic UCM. *Org. Geochem.* **18**, 17–22.
- Gracia E., Charlou J.-L., Radford-Knoery J. and Parson L. M. (2000) Non-transform offsets along the Mid-Atlantic Ridge south of the Azores (38°N–34°N): ultramafic exposures and hosting of hydrothermal vents. *Earth Planet. Sci. Lett.* **177**, 89–103.
- Grice K., Schouten S., Nissenbaum A., Charrach J. and Sinnighe Damsté J. S. (1998) Isotopically heavy carbon in the C<sub>21</sub> to C<sub>25</sub> regular isoprenoids in halite-rich deposits from the Sdom Formation, Dead Sea Basin, Israel. *Org. Geochem.* **28**, 349–359.
- Hansell D. A. (2002) DOC in the global ocean carbon cycle. In *Biogeochemistry of Marine Dissolved Organic Matter* (eds. D. A. Hansell and C. A. Carlson). Academic Press, New York.
- Hansell D. A. and Carlson C. A. (1998) Deep-ocean gradients in the concentration of dissolved organic carbon. *Nature* **395**, 263–266.
- Hart S. R., Blusztajn J. S., Dick H. J. B. and Lawrence J. R. (1994) Fluid circulation in the oceanic crust: contrast between volcanic and plutonic regimes. *J. Geophys. Res.* **99**, 3163–3173.
- Hayes J. M. (1993) Factors controlling <sup>13</sup>C contents of sedimentary organic compounds: principles and evidences. *Mar. Geol.* **113**, 111–125.

- Hayes J. M. (2001) Fractionation of carbon and hydrogen isotopes in biosynthetic pathways. In *Stable Isotope Geochemistry*, vol. 43 (eds. J. W. Valley and D. R. Cole). Reviews in Mineralogy and Geochemistry, pp. 225–278.
- Hedges J. I. (1977) The association of organic molecules with clay minerals in aqueous solutions. *Geochim. Cosmochim. Acta* **41**, 1119–1123.
- Holland H. D. (2002) Volcanic gases, black smokers, and the Great Oxidation Event. *Geochim. Cosmochim. Acta* **66**, 3811–3826.
- Holm N. and Charlou J.-L. (2001) Initial indications of abiogenic formation of hydrocarbons in the Rainbow ultramafic hydrothermal system, Mid-Atlantic Ridge. *Earth Planet. Sci. Lett.* **191**, 1–8.
- Holm N., Cairns-Smith A. G., Daniel R. M., Ferris J. P., Hennem R. J., Shock E. L., Simoneit B. R. and Yanagawa H. (1992) Marine hydrothermal systems and the origin of life: future research. *Orig. Life Evol. Biosph.* **22**, 181–242.
- Holm N., Dumont M., Ivarsson M. and Konn C. (2006) Alkaline fluid circulation in ultramafic rocks and formation of nucleotide constituents: a hypothesis. *Geochim. Trans.*, 1–7.
- Horita J. and Berndt M. E. (1999) Abiogenic methane formation and isotopic fractionation under hydrothermal conditions. *Science* **285**, 1055–1057.
- Kannenbergh E. L. and Poralla K. (1999) Hopanoid biosynthesis and function in bacteria. *Naturwissenschaften* **86**, 168–176.
- Karl D. M. (1995) Ecology of free-living, hydrothermal vent microbial communities. In *The Microbiology of Deep-Sea Hydrothermal Vents* (ed. D. M. Karl). CRC Press Inc., pp. 35–124.
- Karson J. A., Früh-Green G., Kelley D. S., Williams E. A., Yoerger D. R. and Jakuba M. (2006) Detachment shear zone of the Atlantis Massif core complex, Mid-Atlantic Ridge, 30°N. *Geochim. Geophys. Geosyst.* **7**, 1–29.
- Kasting J. F., Egger D. H. and Raeburn S. P. (1993) Mantle redox evolution and the oxidation state of the Archean atmosphere. *J. Geol.* **101**, 245–257.
- Kelley D. S. (1996) Methane-rich fluids in the oceanic crust. *J. Geophys. Res.* **101**, 2943–2962.
- Kelley D. S. (1997) Fluid evolution in slow-spreading environments. *Proc. Ocean Drill. Program, Sci. Results* **153**, 399–415.
- Kelley D. S. and Früh-Green G. L. (1999) Abiogenic methane in deep-seated mid-ocean ridge environments: insights from stable isotope analyses. *J. Geophys. Res.* **104**, 10439–10460.
- Kelley D. S. and Früh-Green G. L. (2000) Volatiles in mid-ocean ridge environment. In *Ophiolites and Oceanic Crust: New Insights From Field Studies and the Ocean Drilling Program*, vol. 349 (eds. Y. E. M. Dilek, E. D. Moores and A. Nicolas). Geological Society of America Special Paper, pp. 237–260.
- Kelley D. S. and Früh-Green G. L. (2001) Volatiles lines of descent in submarine plutonic environments: insights from stable isotope and fluid inclusions analyses. *Geochim. Cosmochim. Acta* **65**, 3325–3346.
- Kelley D. S. and Malpas J. (1996) Melt-fluid evolution in gabbroic rocks from the Hess Deep, Ocean Drilling Leg 147. *Proc. Ocean Drill. Program, Sci. Results* **147**, 213–227.
- Kelley D. S., Karson J. K., Blackam D. K., Früh-Green G. L., Butterfield D. A., Lilley M. D., Olson E. J., Schrenk M. O., Roe K. K., Lebon G. T., Rivizzigno P. and Party A.-S. (2001) An off-axis hydrothermal vent field near the Mid-Atlantic Ridge at 30°N. *Nature* **412**, 145–149.
- Kelley D. S., Lilley M. D. and Früh-Green G. L. (2004) Volatiles in submarine environments: food of life. In *The Subseafloor Biosphere at Mid-ocean Ridges*, vol. 144 (eds. W. S. D. Wilcock, E. F. DeLong, D. S. Kelley, J. A. Baross and S. C. Cary). American Geophysical Union, Washington, DC, pp. 167–189.
- Kelley D. S., Karson J. A., Früh-Green G. L., Yoerger D. R., Shank T. M., Butterfield D. A., Hayes J. M., Schrenk M. O., Olson E. J., Proskurowski G., Jakuba M., Bradley A., Larson B., Ludwig K., Glickson D., Buckman K., Bradley A. S., Brazelton W. J., Roe K., Elend M. J., Delacour A., Bernasconi S. M., Lilley M. D., Baross J. A., Summons R. E. and Sylva S. (2005) A serpentiite-hosted ecosystem: the Lost City Hydrothermal field. *Science* **307**, 1428–1434.
- Krasnov S. G., Cherkashov G. A. and Stepanova T. V., et al. (1995) Detailed geological studies of hydrothermal fields in the North Atlantic. In *Hydrothermal Vents and Processes*, vol. 87 (eds. L. M. Parson, C. L. Walker and D. R. Dixon). Geol. Soc. Spec. Publications, pp. 43–64.
- Lang S. Q., Butterfield D. A., Hedges J. and Lilley M. D. (2005) Production of isotopically heavy dissolved organic carbon in Lost City Hydrothermal Field. *EOS Trans. AGU* **86**, Fall Meet. Suppl., Abstract V43C-06.
- Lang S. Q., Butterfield D. A., Lilley M. D., Johnson H. P. and Hedges J. (2006) Dissolved organic carbon in ridge-axis and ridge-flank hydrothermal systems. *Geochim. Cosmochim. Acta* **70**, 3830–3842.
- de Leeuw J. W., Cox H. C., Van Graas G., van der Meer F. W., Peakman T. M., Baas J. M. A. and Van de Graaf V. (1989) Limited double bond isomerization and selective hydrogenation of sterenes during early diagenesis. *Geochim. Cosmochim. Acta* **53**, 903–909.
- Lilley M. D. et al. (1993) Anomalous CH<sub>4</sub> and NH<sub>4</sub><sup>+</sup> concentrations at an unsedimented mid-ocean-ridge hydrothermal system. *Nature* **364**, 45–47.
- Ludwig K. A., Kelley D. S., Edwards R. L., Shen C.-C. and Cheng H. (2005) U/Th geochronology of carbonate chimneys at the Lost City hydrothermal field. *EOS Trans. AGU* **86**(52), Fall Meet. Suppl., V51B-1487.
- Ludwig K., Kelley D. S., Butterfield D. A., Nelson B. K. and Früh-Green G. (2006) Formation and evolution of carbonate chimneys at the Lost City Hydrothermal Field. *Geochim. Cosmochim. Acta* **70**, 3625–3645.
- Lupton J. E. (1995) Hydrothermal plumes: near and far field. In *Seafloor Hydrothermal Systems: Physical, Chemical, Biological, and Geological Interactions*, vol. 70 (eds. S. E. Humphris, R. A. Zierenberg, L. S. Mullineaux and R. E. Thomson). American Geophysical Union, Washington, DC, pp. 317–346.
- Mackenzie A. S., Brassel S. C., Eglinton G. and Maxwell J. R. (1982) Chemical fossils: the geological fate of steroids. *Science* **217**, 491–504.
- Martin W. and Russel M. J. (2006) On the origin of biochemistry at an alkaline hydrothermal vent. *Phil. Trans. R. Soc.* 1–39. doi:10.1098/rstb.2006.1881.
- Mathez E. A. (1987) Carbonaceous matter in mantle xenoliths: composition and relevance to the isotopes. *Geochim. Cosmochim. Acta* **51**, 2339–2347.
- Mattey D. P., Carr R. H., Wright I. P. and Pillinger C. T. (1984) Carbon isotopes in submarine basalts. *Earth Planet. Sci. Lett.* **70**, 196–206.
- McCullom T. and Seewald J. S. (2001) A reassessment of the potential for reduction of dissolved CO<sub>2</sub> to hydrocarbons during serpentinization of olivine. *Geochim. Cosmochim. Acta* **65**, 3769–3778.
- McCullom T. and Seewald J. S. (2003a) Experimental constraints on the hydrothermal reactivity of organic acids and acid anions: I. Formic acid and formate. *Geochim. Cosmochim. Acta* **67**, 3625–3644.
- McCullom T. and Seewald J. S. (2003b) Experimental study of the hydrothermal reactivity of organic acids and acid anions: II. Acetic acid, acetate, and valeric acid. *Geochim. Cosmochim. Acta* **67**, 3645–3664.

- McCollom T. and Seewald J. S. (2006) Carbon isotope composition of organic compounds produced by abiotic synthesis under hydrothermal conditions. *Earth Planet. Sci. Lett.* **243**, 74–84.
- McCollom T. and Seewald J. S. (2007) Abiotic synthesis of organic compounds in deep-sea hydrothermal environments. *Chem. Rev.* **107**, 382–401.
- Montluçon D. B. and Lee C. (2001) Factors affecting lysine sorption in a coastal sediment. *Org. Geochem.* **32**, 933–942.
- Mottl M. J. (2003) Partitioning of energy and mass flux between midocean ridge axes and flanks at high and low temperature. In *Energy and Mass Transfer in Marine Hydrothermal Systems* (eds. P. E. Halbach, V. Tunnicliffe and J. R. Hein), pp. 271–286.
- Peters K. E. and Moldowan J. M. (1993) *The Biomarker Guide: Interpreting Molecular Fossils in Petroleum and Ancient Sediments*. Prentice-Hall, Englewood Cliffs, New Jersey.
- Pineau F. and Javoy M. (1983) Carbon isotopes and concentrations in mid-oceanic ridge basalts. *Earth Planet. Sci. Lett.* **62**, 239–257.
- Pineau F. and Mathez E. A. (1990) Carbon isotopes in xenoliths from the Hualalai Volcano, Hawaii, and the generation of isotopic variability. *Geochim. Cosmochim. Acta* **54**, 217–227.
- Proskurowski G., Lilley M. D., Kelley D. S. and Olson E. J. (2006) Low temperature volatile production at the Lost City Hydrothermal Field, evidence from a hydrogen stable isotope geothermometer. *Chem. Geol.* **229**, 331–343.
- Proskurowski G., Lilley M. D., Seewald J. S., Früh-Green G. L., Olson E. J., Lupton J. E., Sylva S. P. and Kelley D. S. (2008) Abiogenic hydrocarbon production at Lost City Hydrothermal Field. *Science* **319**, 604–607.
- Rieley G., Coillier R. J., Jones D. M., Eglinton G., Eakin P. A. and Fallick A. E. (1991) Sources of sedimentary lipids deduced from stable carbon-isotopes analyses of individual compounds. *Nature* **352**, 425–427.
- Rieley G., Collister J. W., Stern B. and Eglinton G. (1993) Gas chromatography/isotope ratio mass spectrometry of leaf wax *n*-alkanes from plants of differing carbon dioxide metabolisms. *Rapid Commun. Mass Spectrom.* **7**, 488–491.
- Rishavy M. A. and Cleland W. W. (1999)  $^{13}\text{C}$ ,  $^{15}\text{N}$ , and  $^{18}\text{O}$  equilibrium isotope effects and fractionation factors. *Can. J. Chem.* **77**, 967–977.
- Rona P. A., Widenfalk L. and Bostrom K. (1987) Serpentinized ultramafics and hydrothermal activity at the Mid-Atlantic Ridge crest near 15°N. *J. Geophys. Res.* **92**, 1417–1427.
- Rona P. A., Bougault H., Charlou J.-L., Appriou P., Nelsen T., Trefry J. H., Eberhart G. L., Barone A. and Needham H. D. (1992) Hydrothermal circulation, serpentinization and degassing at a rift valley-fracture zone intersection: Mid-Atlantic Ridge near 15°N, 45W. *Geology* **20**, 783–786.
- Sagalevich A. M., Vinogradov G. M., Gurivich E. G., Lein A. Y., Lukashin V. N. and Chernyaev E. S. (2000) Investigations in the Titanic study area and the Rainbow Hydrothermal Field in Cruise 42 of the Research Vessel Akademik Mstislav Keldysh. *Oceanology* **40**, 439–446.
- Schouten S., Klein Breteler W. C., Blokker P. C., Schogt N., Rijpstra W. I. C., Grice K., Baas M. and Sinninghe Damsté J. S. (1998) Biosynthetic effects on stable carbon isotopic composition of algal lipids: implications for deciphering the carbon isotopic biomarker record. *Geochim. Cosmochim. Acta* **62**, 1397–1406.
- Schroeder T. and John B. E. (2004) Strain localization on an oceanic detachment fault system, Atlantis Massif, 30°N, Mid-Atlantic Ridge. *Geochem. Geophys. Geosyst.* **5**. doi:10.1029/2004GC000728.
- Schroeder T., John B. and Frost B. R. (2002) Geologic implications of seawater circulation through peridotite exposed at slow-spreading mid-ocean ridges. *Geology* **30**, 367–370.
- Schwarzenbach R. P., Gschwend P. M. and Imboden D. M. (2003) *Environmental Organic Chemistry*, second ed. Wiley, Hoboken, NJ.
- Shanks, III, W. C., Bohlke J. K. and Seal, II, R. R. (1995) Stable isotopes in mid-ocean ridge hydrothermal systems: interactions between fluids, minerals, and organisms. In *Seafloor Hydrothermal Systems: Physical, Chemical, Biological, and Geological Interactions*, vol. 70 (eds. S. E. Humphris, R. A. Zierenberg, L. S. Mullineaux and R. E. Thomson). American Geophysical Union, Washington, DC, pp. 194–221.
- Shock E. L. (1990) Geochemical constraints on the origin of organic compounds in hydrothermal systems. *Orig. Life Evol. Biosph.* **20**, 331–367.
- Shock E. L. and Schulte M. D. (1998) Organic synthesis during fluid mixing in hydrothermal systems. *J. Geophys. Res.* **103**, 28513–28527.
- Simoneit B. R. T., Lein A. L., Peresypkin V. I. and Osipov G. A. (2004) Composition and origin of hydrothermal petroleum and associated lipids in the sulfide deposits of the Rainbow field (Mid-Atlantic ridge at 36°N). *Geochim. Cosmochim. Acta* **68**, 2275–2294.
- Staudigel H., Hart S. R., Schmincke H. U. and Smith B. M. (1989) Cretaceous ocean crust at DSDP Sites 417 and 418: carbon uptake from weathering versus loss by magmatic outgassing. *Geochim. Cosmochim. Acta* **53**, 3091–3094.
- Svensson E., Skoog A. and Amend J. P. (2004) Concentration and distribution of dissolved amino acids in shallow hydrothermal system, Vulcano Island (Italy). *Org. Geochem.* **35**, 1001–1014.
- Sugisaki R. and Mimura K. (1994) Mantle hydrocarbons: abiotic or biotic? *Geochim. Cosmochim. Acta* **58**, 2527–2542.
- ten Haven H. L., de Leeuw J. W., Sinninghe Damsté J. S., Schenk P. A., Palmer S. E. and Zumberge J. E. (1988) Application of biological markers in the recognition of paleohypersaline environments. In *Lacustrine Petroleum Source Rocks*, vol. 40 (eds. A. J. Fleet, K. Kelts and m. R. Talbot). Geol. Soc. Spec. Pub., pp. 123–130.
- Tornabene T. G., Langworthy T. A., Holzer G. and Oro J. (1979) Squalenes, phytanes and other isoprenoids as major neutral lipids of methanogenic and thermoacidophilic “Archaeobacteria”. *J. Mol. Evol.* **13**, 73–83.
- Volkman J. K. (2006) Lipids markers for marine organic matter. In *Marine Organic Matter: Biomarkers, Isotopes and DNA* (ed. J. K. Volkman). Springer, Berlin, pp. 27–70.
- Volkman J. K. and Maxwell J. R. (1986) Acyclic isoprenoids as biological biomarkers. In *Biological Markers in Sedimentary Record* (ed. R. B. Johns). Elsevier, New York, pp. 1–42.
- Wang X.-C. and Lee C. (1993) Adsorption and desorption of aliphatic amines, amino acids and acetate by clay minerals and marine sediments. *Mar. Chem.* **44**, 1–23.
- Zeebe R. E. and Wolf-Galdrow D. (2001)  $\text{CO}_2$  in seawater: equilibrium, kinetics, isotopes. Elsevier Oceanography Series, **65**, p. 346.

Associate editor: Jeffrey Seewald